NEUROSCIENCE
RESEARCH ARTICLE

INTERNATIONAL BRAIN IBRO RESEARCH ORGANIZATION

P. Andrés-Benito et al. / Neuroscience xxx (2021) xxx–xxx

Dysregulated Protein Phosphorylation as Main Contributor of Granulovacuolar Degeneration at the First Stages of Neurofibrillary Tangles Pathology

Pol Andrés-Benito,[a] Margarita Carmona,[a] Mónica Jordán Pirla,[a] Benjamín Torrejón-Escribano,[b] José Antonio del Rio[c,d] and Isidro Ferrer[a]*

[a] *Department of Pathology and Experimental Therapeutics, University of Barcelona, CIBERNED (Network Centre of Biomedical Research of Neurodegenerative Diseases), Institute of Health Carlos III, Bellvitge University Hospital/Bellvitge Biomedical Research Institute (IDIBELL), Hospitalet de Llobregat, Barcelona, Spain*

[b] *Advanced Light Microscopy Unit (Campus de Bellvitge), Scientific and Technical Facility (CCiTUB), University of Barcelona, Hospitalet de Llobregat, Spain*

[c] *Molecular and Cellular Neurobiotechnology, Institute of Bioengineering of Catalonia (IBEC), Barcelona Institute for Science and Technology, Science Park Barcelona (PCB), Barcelona, Spain*

[d] *Department of Cell Biology, Physiology and Immunology, Faculty of Biology, University of Barcelona, Spain*

Abstract—The hippocampus of cases with neurofibrillary tangles (NFT) pathology classified as stages I–II, III–IV, and V–VI without comorbidities, and middle-aged (MA) individuals with no NFT pathology, were examined to learn about the composition of granulovacuolar degeneration (GVD). Our results confirm the presence of CK1-δ, p38-P Thr180/Tyr182, SAPK/JNK-P Thr183/Thr185, GSK-3α/β-P Tyr279/Tyr216, and GSK-3β Ser9 in the cytoplasmic granules in a subset of neurons of the CA1 and CA2 subfields of the hippocampus. Also, we identify the presence of PKA α/β-P Thr197, SRC-P Tyr416, PAK1-P Ser199/Ser204, CAMK2A-P Tyr197, and PKCG-P Thr655 in cytoplasmic granules in cases with NFT pathology, but not in MA cases. Our results also confirm the presence of β-catenin-P Ser45/Thr41, IREα-P Ser274, eIF2α-P Ser51, TDP-43-P Ser403-404 (but absent TDP-43), and ubiquitin in cytoplasmic granules. Other components of the cytoplasmic granules are MAP2-P Thr1620/1623, MAP1B-P Thr1265, ADD1-P Ser726, and ADD1/ADD1-P Ser726/Ser713, in addition to several tau species including 3Rtau, 4Rtau, and tau-P Ser262. The analysis of GVD at progressive stages of NFT pathology reveals the early appearance of phosphorylated kinases and proteins in cytoplasmic granules at stages I–II, before the appearance of pre-tangles and NFTs. Most of these granules are not surrounded by LAMP1-positive membranes. Markers of impaired ubiquitin-protesome system, abnormal reticulum stress response, and altered endocytic and autophagic pathways occur in a subpopulation of neurons containing cytoplasmic granules, and they appear later. These observations suggest early phosphorylation of kinases leading to their activation, and resulting in the abnormal phosphorylation of various substrates, including tau, as a main alteration at the first stages of GVD.

Key words: granulovacuolar degeneration, brain aging, Alzheimer's disease, tau, protein phosphorylation, kinases.

INTRODUCTION

Sporadic Alzheimer's disease (sAD) is a biological process, progressive with aging, characterized by the presence of neurofibrillary tangles (NFTs) and senile plaques (SPs) distributed throughout the brain with a distinctive pattern (Braak and del Tredici, 2011; Ferrer, 2012).

The main constituent of NFTs in sAD is a combination of all six hyper-phosphorylated brain tau isoforms with a variable almost equal proportion of 3Rtau and 4Rtau isoforms (Goedert et al., 1988; Goedert et al., 1992; Buée et al., 2000; Iqbal et al., 2005; Hernández and Avila, 2007; Spillantini and Goedert, 2013). The study of consecutive series of the current population recognizes six stages of NFT pathology involving selected nuclei of the telencephalon and the brainstem (Braak and Braak, 1991; Braak and Braak, 1995; Braak et al., 2011; Braak and Del Tredici, 2015). About 85% of individuals aged

*Corresponding author at: Department of Pathology and Experimental Therapeutics, University of Barcelona, Feixa Llarga sn, 08907 Hospitalet de Llobregat, Spain.
E-mail addresses: pandres@idibell.cat (P. Andrés-Benito), mcarmona@idibell.cat (M. Carmona), mjordanpirla@gmail.com (M. J. Pirla), torrejonbenja@ub.edu (B. Torrejón-Escribano), jadelrio@ibecbarcelona.eu (J. A. del Rio), 8082ifa@gmail.com (I. Ferrer).

https://doi.org/10.1016/j.neuroscience.2021.10.023
0306-4522/

Please cite this article in press as: Andrés-Benito P et al. Dysregulated Protein Phosphorylation as Main Contributor of Granulovacuolar Degeneration at the First Stages of Neurofibrillary Tangles Pathology. Neuroscience (2021), https://doi.org/10.1016/j.neuroscience.2021.10.023

65 have NFT pathology, at least restricted to stages I–III (Braak and Del Tredici, 2011; Ferrer, 2012; Ferrer and Andrés-Benito, 2020). Most of them are cognitively normal and the neuropathological changes are considered in the context of normal brain aging. Cases at middle stages (stages III–IV), in which there is involvement of the hippocampus and limbic system, may show mild cognitive impairment or not suffer any apparent cognitive defect. Cases at stages V–VI (advanced stages) in which almost all the telencephalon and basal ganglia are filled with NFTs suffer from clinical sAD (Nelson et al., 2012).

The main constituent of SPs is β-amyloid, which is also the main component of diffuse plaques and β-amyloid angiopathy. β-Amyloid deposition also increases with disease progression following defined patterns (Braak and Braak, 1991; Thal et al., 2002). The majority of individuals at stages I–II and about of those at stage III do not have SPs or β-amyloid deposits (Braak et al., 2011; Ferrer, 2012; Ferrer and Andrés-Benito, 2020). Increased numbers of SPs are common accompanying stages III–IV onwards.

In addition to these two major hallmarks of AD, other lesions are consistently present including Hirano bodies and granulovacuolar degeneration (GVD). Hirano bodies are eosinophilic, rod-shape inclusions derived from an abnormal organization of the neuronal cytoskeleton (Galloway et al., 1987). GVD is characterized by the presence of vacuolar cytoplasmic lesions with a dense central core. GVD first appears in neurons of the hippocampal subfields CA1 and CA2, and the subiculum; this is followed by the entorhinal cortex, and CA4 neurons in stage 2, temporal neocortex in stage 3, amygdala and/or the hypothalamus in stage 4, and cingulate, frontal, and parietal cortices in stage five (Thal et al., 2011).

Tau hyper-phosphorylation is a determining factor in the formation of NFTs. Phosphorylation is one of the most common and essential mechanisms of protein function. This posttranslational modification mostly derives from activation/inhibition of protein function and/or recruitment of interacting proteins with structurally conserved domains. In the context of AD, tau hyperphosphorylation is a paradigm of altered protein phosphorylation. However, robust phosphoproteomics studies have identified a large number of phosphorylated proteins in addition to tau at advanced stages of AD (Tan et al., 2015; Triplett et al., 2016; Rudrabhatla et al. 2011; Zahid et al., 2012; Dammer et al., 2015; Tagawa et al., 2015; Chen et al., 2019; Sathe et al., 2020; Drummond et al., 2020). We analyzed the expression of phosphoproteins in the entorhinal cortex and frontal cortex in cases with NFT pathology at stages I–II, III–IV, and V–VI without co-morbidities in comparison with middle-aged (MA) individuals without NFTs. A major point was the identification of 214 dysregulated phosphoproteins in the EC, of which 65 were dysregulated at the first stages (I–II); 167 phosphoproteins were dysregulated in the FC, 81 of them at stages I–II (Ferrer et al., 2021). Therefore, aberrant phosphorylation appears with brain aging at first stages of AD.

The objective of the present study is to assess the cellular localization of selected dysregulated phosphoproteins in the hippocampus of the same group of cases as those examined using (phospho)proteomics (Ferrer et al., 2021), and their expression in particular compartments including granules and GVD, pre-tangles and NFTs, dystrophic neurites (DNs) surrounding SPs, and neuropil threads (NTs). We also analyze the localization of a subset of proteins with a focus on GVD in an attempt to learn about its pathogenesis and possible functional implications.

EXPERIMENTAL PROCEDURES

Tissue samples

Post-mortem samples were obtained from the Institute of Neuropathology HUB-ICO-IDIBELL Biobank following the guidelines of Spanish legislation on this matter and the approval of the local ethics committee (CEIC) of the Bellvitge University Hospital. The post-mortem interval between death and tissue processing was between 3 h and 11 h 15 min. One hemisphere was immediately cut in coronal sections, 1-cm thick, and selected areas of the encephalon were rapidly dissected, frozen on metal plates over dry ice, placed in individual air-tight plastic bags, numbered with water-resistant ink, and stored at −80 °C until used for biochemical studies. The other hemisphere was fixed by immersion in 4% buffered formalin for 3 weeks for morphologic study. Transversal sections of the spinal cord were alternatively frozen at −80 °C or fixed by immersion in 4% buffered formalin. The neuropathological study was carried out on paraffin sections of twenty-five selected regions of the cerebrum, cerebellum, brain stem, and spinal cord which were stained with hematoxylin and eosin, Klüver-Barrera, and periodic acid Schiff, or processed for immunohistochemistry with anti-β-amyloid, phospho-tau (clone AT8), α-synuclein, αB-crystallin, TDP-43, TDP-43-P, ubiquitin, p62, glial fibrillary acidic protein, CD68, and IBA1 antibodies (Ferrer et al., 2008; Ferrer, 2014).

Pathological cases (n = 15) were those having NFT Braak stages I–II (n = 5; 3 male, 2 women, 68.8 ± 10.9 years), III–IV (n = 5; 4 male, 1 female, 77.2 ± 5.7 years), and V–VI (n = 5; 81 ± 7.5 years). Cases with associated pathology including other tauopathies, α-synucleinopathy, TDP-43 proteinopathy, other neurodegenerative diseases, vascular diseases, and neoplastic diseases affecting the nervous system were excluded. In addition, patients with arterial hypertension, type II diabetes, morbid obesity, hyperlipidemia, hepatic failure, renal failure, respiratory insufficiency, metabolic syndromes, and prolonged axonal states such as those occurring in intensive care units were excluded. Cases with infectious, inflammatory, or autoimmune diseases, either systemic or limited to the nervous system, were not included. Middle-aged (MA) control cases (n = 9; 5 men, 4 women; 58.8 ± 12.3 years) had not suffered from neurologic or psychiatric diseases and did not have abnormalities in the neuropathological examination including the absence of NFTs (Ferrer et al., 2021).

Supplementary Table 1 summarizes the characteristics of cases used in this series. NFT pathology was categorized according to the staging of

Please cite this article in press as: Andrés-Benito P et al. Dysregulated Protein Phosphorylation as Main Contributor of Granulovacuolar Degeneration at the First Stages of Neurofibrillary Tangles Pathology. Neuroscience (2021), https://doi.org/10.1016/j.neuroscience.2021.10.023

Braak and Braak (1991) modified for paraffin sections (Braak et al., 2006), β-amyloid deposits according to Thal phases (Thal et al., 2002), and CERAD scores according to the National Institute on Aging-Alzheimer's Association guidelines for the neuropathologic assessment of Alzheimer's disease (Hyman et al., 2012; Montine et al., 2012). Additionally, cases 12 and 14, which were categorized as phase A1 of Thal, had diffuse plaques in the frontal cortex but not in the entorhinal cortex.

Immunohistochemistry and double-labeling immunofluorescence and confocal microscopy

The selection of the antibodies was based on the list of phosphoproteins identified in a previous (phospho) proteomics study in the entorhinal cortex and frontal cortex area 8 at different stages of NFT pathology (Ferrer et al., 2021). The cases assessed in that work are the same as those analyzed in the present study. All MS raw data and search result files have been deposited at the ProteomeXchange Consortium (http://proteomecentral.proteomexchange.org) via the PRIDE partner repository with the dataset identifiers PXD021645 (Reviewer account details: Username: reviewer_pxd021645@ebi.ac.uk; Password: ANBskoaI) and PXD021653 (Reviewer account details: Username: reviewer_pxd021653@ebi.ac.uk; Password: kMAyoOkq). In addition, other antibodies that recognize well-established components of GVD are used for comparison and validation purposes.

Paraffin-embedded, 4 μm-thick de-waxed paraffin sections of the anterior and posterior hippocampus were boiled in citrate buffer (20 min) to retrieve protein antigenicity. Endogenous peroxidases were blocked by incubation in 10% methanol-1% H_2O_2 solution (15 min) followed by 3% normal horse serum solution. Then the sections were incubated at 4 °C overnight with one of the primary antibodies listed in Supplementary Table 2. Following incubation with the primary antibody, the sections were incubated with EnVision + system peroxidase (Dako, Agilent Technologies, Santa Clara, CA, USA) for 30 min at room temperature. The peroxidase reaction was visualized with diaminobenzidine and H_2O_2. Control of the immunostaining included omission of the primary antibody; no signal was obtained following incubation with only the secondary antibody.

For double-labeling immunofluorescence and confocal microscopy, de-waxed sections, 4 μm thick, were stained with a saturated solution of Sudan black B (Merck, Glostrup, DE) for 15 min to block the autofluorescence of lipofuscin granules present in cell bodies, and then rinsed in 70% ethanol and washed in distilled water. The sections were incubated at 4 °C overnight with combinations of primary antibodies. The characteristics of the antibodies are listed in Supplementary Table 2. After washing, the sections were incubated with Alexa488 or Alexa546 (1:400, Molecular Probes, Eugene, OR, USA) fluorescence secondary antibodies against the corresponding host species. Nuclei were stained with DRAQ5™ (dilution 1:2000, BioStatus, Loughborough, UK). After washing, the sections were mounted in Immuno-Fluore mounting medium (ICN Biomedicals, Irvine, CA, USA), sealed, and dried overnight. Sections were examined with a Leica TCS-SL confocal microscope (Ferrer et al., 2014).

Semi-quantitative evaluation

Semi-quantitative assessment of optical microscopy sections was carried out in AD cases stage V–VI. The number of immunoreactive neurons with GVD and NFTs positive with the different antibodies was counted in three areas of the CA1 region at a magnification of ×400 selected at random in a given section in every case. Serial sections, one of them stained with haematoxylin and eosin, were used for this purpose. The total number of neurons in selected areas was counted in the section stained with haematoxylin and eosin. The number of immunoreactive neurons with every antibody was expressed as the percentage of the total number of neurons in these areas. The expression of positive neurons was eventually listed semi-quantitatively considering the median values in AD stage V–VI. The following signs were used as final indicators; values for GVD, +++: 20–30% of the total number of neurons; ++: 10–19; +: 1–9%; +/−: not present in all sections; values for NFT, ###: 50–70%; ##: 20–49%; #: 1–19%; #/-: not present in all sections. The evaluation of immunoreactivty in dystrophic neurites of SPs and neuropil threads expressed as §§§, §§, §, – indicate abundant, moderate number, rarely stained, or not stained at all, respectively.

RESULTS

The study was centred on the CA1 and CA2 subfields of the hippocampus in MA and in cases with progressive stages of NFT pathology (stages I–II, III–IV, and V–VI) with no associated pathologies. Special attention was paid to the localization of phosphorylated kinases and other phosphorylated proteins in comparison to common markers of GVD, NFTs, DNs, and NTs.

Phosphorylated kinases

p38-P Thr180/tyr182 (p38-P) immunoreactivity was first observed at stages I–II of NFT pathology in abundant cytoplasmic granules in a subpopulation of CA1 and CA2 neurons. The number of neurons with cytoplasmic granules increased at the middle and advanced stages of NFT pathology. In contrast, only a few pre-tangles and rare NFTs were stained with anti-p38-P antibodies, some of them also containing cytoplasmic granules. p38-P was one of the best markers of cytoplasmic granules across the NFT staging (Fig. 1A). DNs and NTs were rarely stained with anti-p38-P antibodies.

A different pattern was found for stress-activated protein kinase/Jun amino-terminal kinase Thr183/Thr185 (SAPK/JNK-P) immunoreactivity. No positive structures were present in MA cases. SAPK/JNK-P-positive cytoplasmic granules were found in a few neurons of the CA1 and CA2 subfields. In contrast, pre-tangles and NFTs showed strong SAPK/JNK-P-immunoreactivity

Please cite this article in press as: Andrés-Benito P et al. Dysregulated Protein Phosphorylation as Main Contributor of Granulovacuolar Degeneration at the First Stages of Neurofibrillary Tangles Pathology. Neuroscience (2021), https://doi.org/10.1016/j.neuroscience.2021.10.023

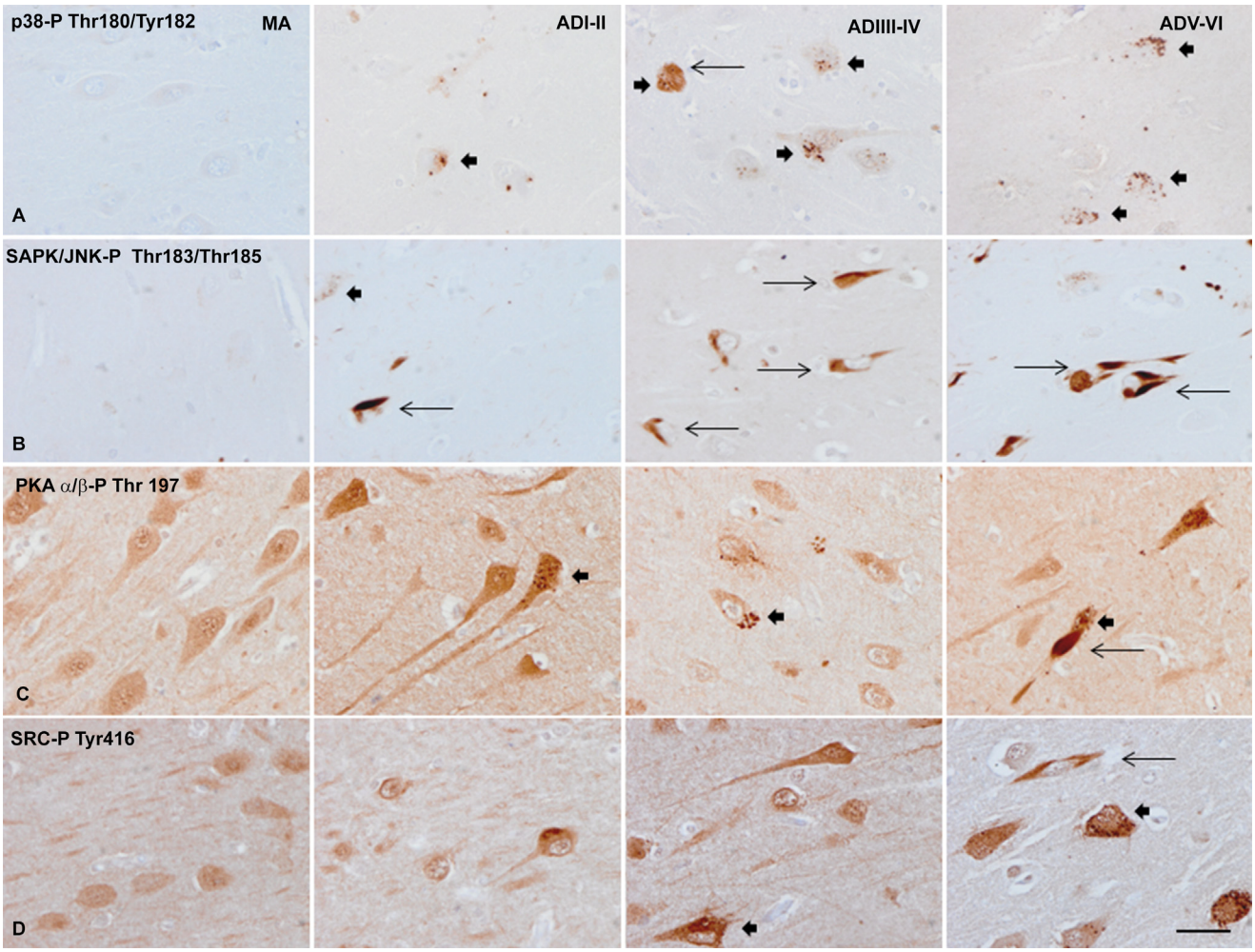

Fig. 1. Immunohistochemistry of phosphorylated kinases p38-P Thr180/Tyr182, SAPK/JNK-P Thr183/Thr185, PKA α/β-P Thr197, and SRC-P Tyr 416 in the CA1 area of the hippocampus in middle-aged cases (MA), and at stages I–II, III–IV, and V–VI of NFT pathology. **(A)** p-38-P immunoreactivity is found in cytoplasmic granules of a subset of neurons (thick arrows), and in fibrillary cytoplasmic deposits (thin arrows). Both lesions may be seen in the same neuron. **(B)** SAPK/JNK-P is found predominantly in cytoplasmic deposits consistent with NFTs (thin arrows); neurons with cytoplasmic granules (thick arrow) are scanty when compared with parallel sections stained with anti-p38-P antibodies. The morphology of the inclusion at stage I–II resembles a Hirano body but it showed a characteristic NFT morphology in an immediate section stained with the AT8 antibody. **(C)** PKA α/β-P immunoreactivity decorates the cytoplasm of neurons in MA and NFT cases. Cytoplasmic PKA α/β-P is reduced with NFT staging, but strong PKA α/β-P-positive granules (thick arrows), and immunoreactive deposits consistent with NFTs (thin arrows) appear in the cytoplasm in a subset of neurons with NFT stage progression. **(D)** SRC-P immunoreactivity occurs in the cytoplasm of neurons in MA and pathological cases. Strong SRC-P immunostaining identifies a few neurons with cytoplasmic granules (thick arrows), or with elongated deposits consistent with pre-tangles or tangles (long arrows). Note the early appearance of cytoplasmic granules in comparison to the late formation of NFT-like deposits. Paraffin sections, lightly counterstained with hematoxylin, bar = 50 μm.

along with disease progression (Fig. 1B). DNs and NTs were stained with anti-SAPK/JNK-P antibodies.

Weak protein kinase A or cyclic AMP-dependent protein kinase A Thr197 (PKA α/β-P) immunoreactivity decorated the nucleus and cytoplasm of CA1 and CA2 hippocampal neurons in MA and NFT cases. Also, PKA α/β-P immunoreactivity recognized cytoplasmic granules in selected neurons in the CA1 and CA2 areas of the hippocampus at the first stages (I–II) of NFT pathology, increasing in number at the middle stages (III–IV). Some NFTs and pre-tangles were immunostained with anti-PKA α/β-P antibodies; a few neurons contained both PKA α/β-P-positive cytoplasmic granules and NFTs (Fig. 1C). DNs and NTs were negative.

Anti-tyrosine-protein kinase SRC Tyr416 (SRC-P) antibodies weakly decorated the nucleus and cytoplasm of neurons in MA and NFT cases. Also, neurons with cytoplasmic granules, and subpopulations of pre-tangles and NFTs, were immunostained with anti-SRC-P antibodies across NFT staging. However, many neurons with GVD, as revealed by hematoxylin counterstaining, were devoid of SRC-P-positive granules. Moreover, SRC-P immunoreactivity was decreased in the cytoplasm of some neurons at stages V–V when compared with MA cases (Fig. 1D). DNs and NTs were negative with anti-SRC-P antibodies.

Serine threonine protein kinase 1 Ser199/Ser204 (PAK1-P) immunoreactivity was localized in the nucleus

Please cite this article in press as: Andrés-Benito P et al. Dysregulated Protein Phosphorylation as Main Contributor of Granulovacuolar Degeneration at the First Stages of Neurofibrillary Tangles Pathology. Neuroscience (2021), https://doi.org/10.1016/j.neuroscience.2021.10.023

of neurons in MA and NFT cases. Granular cytoplasmic inclusions and NFTs were strongly immunostained with anti-PAK1-P antibodies. The number of labeled neurons in the CA1 and CA2 subfields increased with NFT stage progression (Fig. 2A). DNs and NTs were negative with anti-PAK-1 antibodies.

No calcium-calmodulin kinase 2A Tyr786 (CAMK2A-P) immunostaining was observed in MA cases. However, abundant CAMK2A-P-positive cytoplasmic granules appeared in CA1 and CA2 neurons at stages I–II; the number of affected neurons increased at stages III–IV and V–VI. NFTs were negative with this antibody at all stages (Fig. 2B). DNs and NTs were not stained with anti-CAMK2A-P antibodies.

Neurons of the CA1 and CA2 subfields in MA cases, and at different NFT stages showed weak cytoplasmic protein kinase C γ type Thr655 (PKCG-P) immunoreactivity. A subpopulation of neurons in the CA1 and CA2 subfields evidenced strong PKCG-P immunoreactivity in cytoplasmic granules. NFTs were negative (Fig. 2C). DNs and NTs were not stained with anti-PKCG-P antibodies.

The antibody GSK α/β-P recognized glycogen synthase kinase 3 α phosphorylated at Tyr279 and β at Tyr216. Antibodies against GSK 3α/β-P stained cytoplasmic granules in a subpopulation of CA1 and CA2 neurons. NFTs were weakly-labelled with the antibody GSK-P Tyr279/Tyr216 (Ferrer et al., 2002) (data not shown). The anti-phospho-specific GSK-3β-P Ser9 antibody decorated NFTs, DNs, and NPs (Ferrer et al., 2002, 2005). Cytoplasmic granules were also immunostained with anti-GSK-3β-P Ser9 antibodies in our study (Fig. 2D).

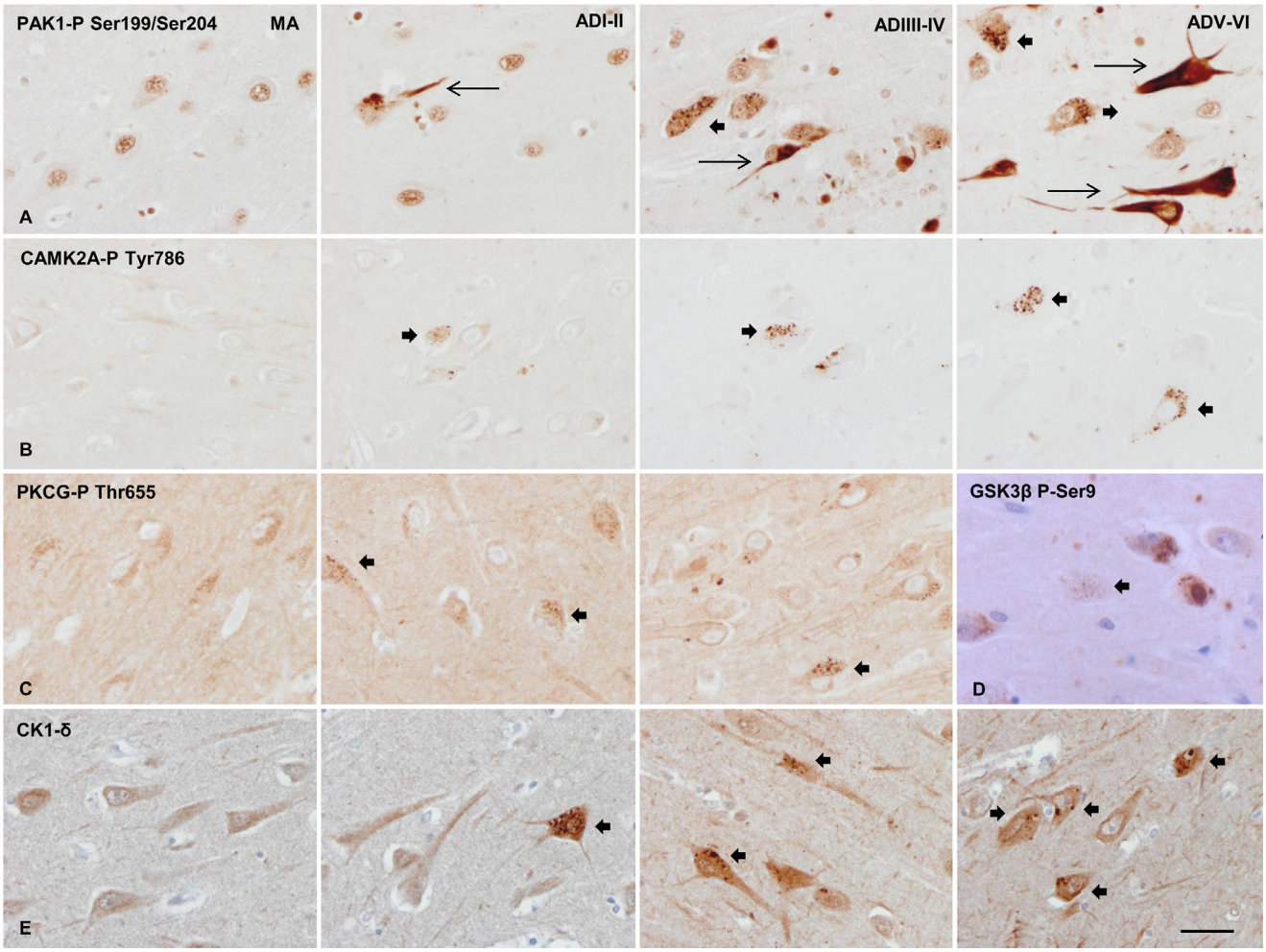

Fig. 2. Immunohistochemistry of phosphorylated kinases PAK1-P Ser199/Ser204, CAMK2A-P Tyr 786, PKCG-P THr655, and CK1-δ in the CA1 area of the hippocampus in MA, and at stages I–II, III–IV, and V–VI of NFT pathology. **(A)** PAK1-P decorates the nuclei of neurons in MA and pathological cases. Cytoplasmic granules of selected neurons (thick arrows) and inclusions reminiscent of NFTs (thin arrows) show strong PAK1-P immunoreactivity. **(B)** CAMK2A-P antibodies stain cytoplasmic granules in a subset of hippocampal neurons (thick arrows). **(C)** PKCG-P immunoreactivity shows a similar pattern. Positive granules (thick arrows) are seen in a subset of neurons. Structures mimicking NFTs are not stained with anti-PKCG-P antibodies. The characteristics of the staining at stages V–VI are similar to those seen at stages III/IV and were skipped in the figure. **(D)** GSK 3β-P Ser9 immunoreactivity showing positive cytoplasmic granules within vacuoles (thick arrow) in AD stage V–VI. **(E)** Neuronal cytoplasmic granules, often located within a vacuole, strongly immunostained with anti-CK1-δ antibodies. Paraffin sections, lightly counterstained with hematoxylin, bar = 50 μm.

Please cite this article in press as: Andrés-Benito P et al. Dysregulated Protein Phosphorylation as Main Contributor of Granulovacuolar Degeneration at the First Stages of Neurofibrillary Tangles Pathology. Neuroscience (2021), https://doi.org/10.1016/j.neuroscience.2021.10.023

Other phosphorylated proteins

The antibody AT8 (anti-tau-P Ser202/Thr205) and phospho-tau specific anti-tau-P Thr181 antibody decorated pre-tangles, NFTs, DNs, and NTs, but not GVD. In contrast, the antibody tau-P Ser262 decorated cytoplasmic granules of a subpopulation of CA1 and CA2 neurons, in addition to NFTs, DNs, and NTs (Fig. 3A).

Neurons with pre-tangles and NFTs showed MAP2-P Thr1620/1623 immunoreactivity. Also, MAP2-P-positive granules were present in neurons at pre-tangle stages (Fig. 3B). The pattern of sections stained with MAP2-P antibodies was similar to that seen in parallel sections stained with the antibody AT8 (excepting the negative AT8 staining of cytoplasmic granules).

In contrast to MAP2-P, MAP1B-P Thr1265 immunoreactivity decorated the nuclei of neurons in MA and NFT cases. Moreover, a subpopulation of CA1 and CA2 neurons displayed cytoplasmic granules with strong MAP1B-P immunoreactivity at stages I–II of NFT pathology. The number of cells with positive granules increased at the middle and advanced stages. NFTs, DNs, and NTs were negative with anti-MAP1B-P antibodies (Fig. 3C).

Rare positive fibers showed NFL-P Ser473 immunoreactivity in MA cases. A few neurons with NFTs were stained at different NFT stages. However, the number of NFL-P-positive neurons was by far smaller than the number of NFTs recognized with AT8 and anti-MAP2-P antibodies (Fig. 3D).

The hippocampus of MA individuals was negative with anti-catenin β-P Ser45/Thr41 antibodies. However, numerous catenin β-P-immunoreactivity cytoplasmic granules decorated a subpopulation of CA1 and CA2 neurons at the first stages of NFT pathology. The number of affected neurons increased at stages III–IV together with the appearance of catenin-β-P-

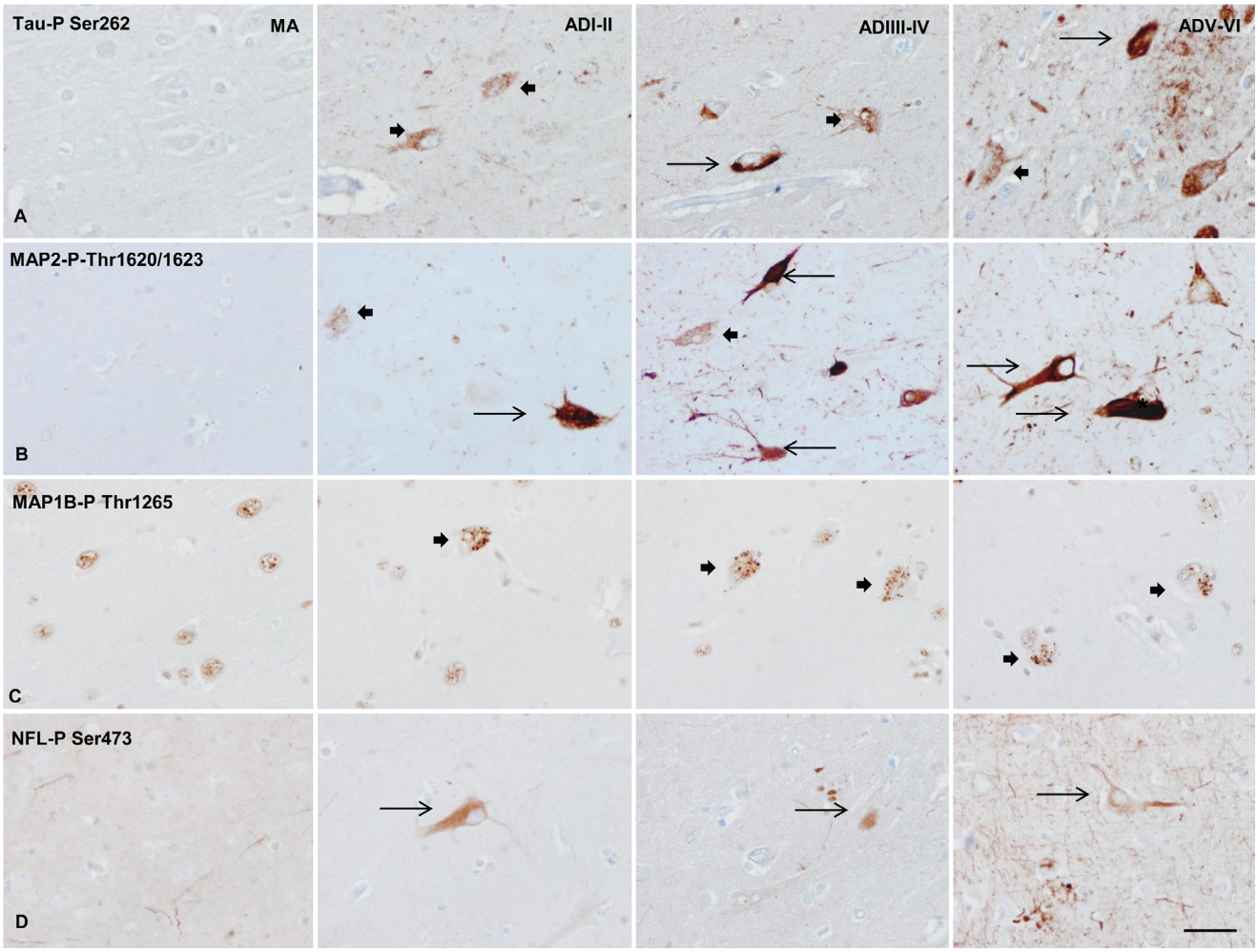

Fig. 3. Immunohistochemistry of phosphorylated proteins tau-P-Ser262, MAP2-P Thr1620/1623, MAP1B-P Thr1265, and NFL-P Ser473 in the CA1 area of the hippocampus in (MA, and at stages I–II, III–IV, and V–VI of NFT pathology. [Where is A?] **(B)** MAP2-P immunoreactivity occurs in cytoplasmic granules (thick arrows), and cytoplasmic fibrillary inclusions consistent with NFTs (thin arrows). Neuropil threads are also decorated with anti-MAP2-P antibodies. Note the early appearance of granular cytoplasmic inclusions in comparison with the late formation of NFT-like inclusions. **(C)** MAP1B-P immunoreactivity decorates cytoplasmic granules in a subset of neurons (thick arrows). NFTs are not stained with this antibody. **(D)** NFL-P immunostaining is not found in cytoplasmic granules but is found in a few neurons with deposits resembling pre-tangles (thin arrows). Paraffin sections, lightly counterstained with hematoxylin, bar = 50 μm.

Please cite this article in press as: Andrés-Benito P et al. Dysregulated Protein Phosphorylation as Main Contributor of Granulovacuolar Degeneration at the First Stages of Neurofibrillary Tangles Pathology. Neuroscience (2021), https://doi.org/10.1016/j.neuroscience.2021.10.023

immunoreactive NFTs. The number of neurons with cytoplasmic granules was maintained or even decreased at stages V–VI in parallel to the increase in the number of positive NFTs in the same regions (Fig. 4A). DNs and NTs were negative.

Weak adducin1-P Ser726 (ADD1-P) immunoreactivity decorated the cytoplasm of neurons in MA cases. ADD1-P-positive cytoplasmic granules appeared in a few neurons in the CA1 and CA2 subfields at stages I–II. The number of neurons with granules increased at stages III–IV, and decreased at stages V–VI. This occurred in parallel to the appearance of ADD1-P-immunoreactive NFTs, and with the presence of ADD1-P-positive astrocytes (Fig. 4B). DNs and NTs were negative. ADD1/ADD2-P Ser726/Ser713 antibodies showed the same pattern of staining. Abundant ADD1/ADD2-P-positive cytoplasmic granules were found in a subpopulation of CA1 and CA2 neurons at stages I–II. The number of neurons with granules increased at stages III–IV, only to decrease thereafter. In contrast, the number of ADD1/ADD2-P-positive NFTs and astrocytes increased with the stage progression (Fig. 4C). DNs and NTs were negative. Diffuse plaques were labeled with anti-ADD1-P and anti-ADD1/ADD2-P antibodies; the staining was likely related to fine astrocyte processes (data not shown).

The antibody anti-TDP43-P Ser403-404 decorated cytoplasmic granules in a subset of neurons in the CA1 and CA2 subfields at different AD stages (Fig. 4D, E). NFTs, DNs, and NTs were negative.

The antibody anti-phosphorylated inositol-requiring enzyme 1α (IRE1α-P Ser274) immunostained cytoplasmic granules, often located within a vacuole, in a subset of CA1 and CA2 neurons in NFT cases more

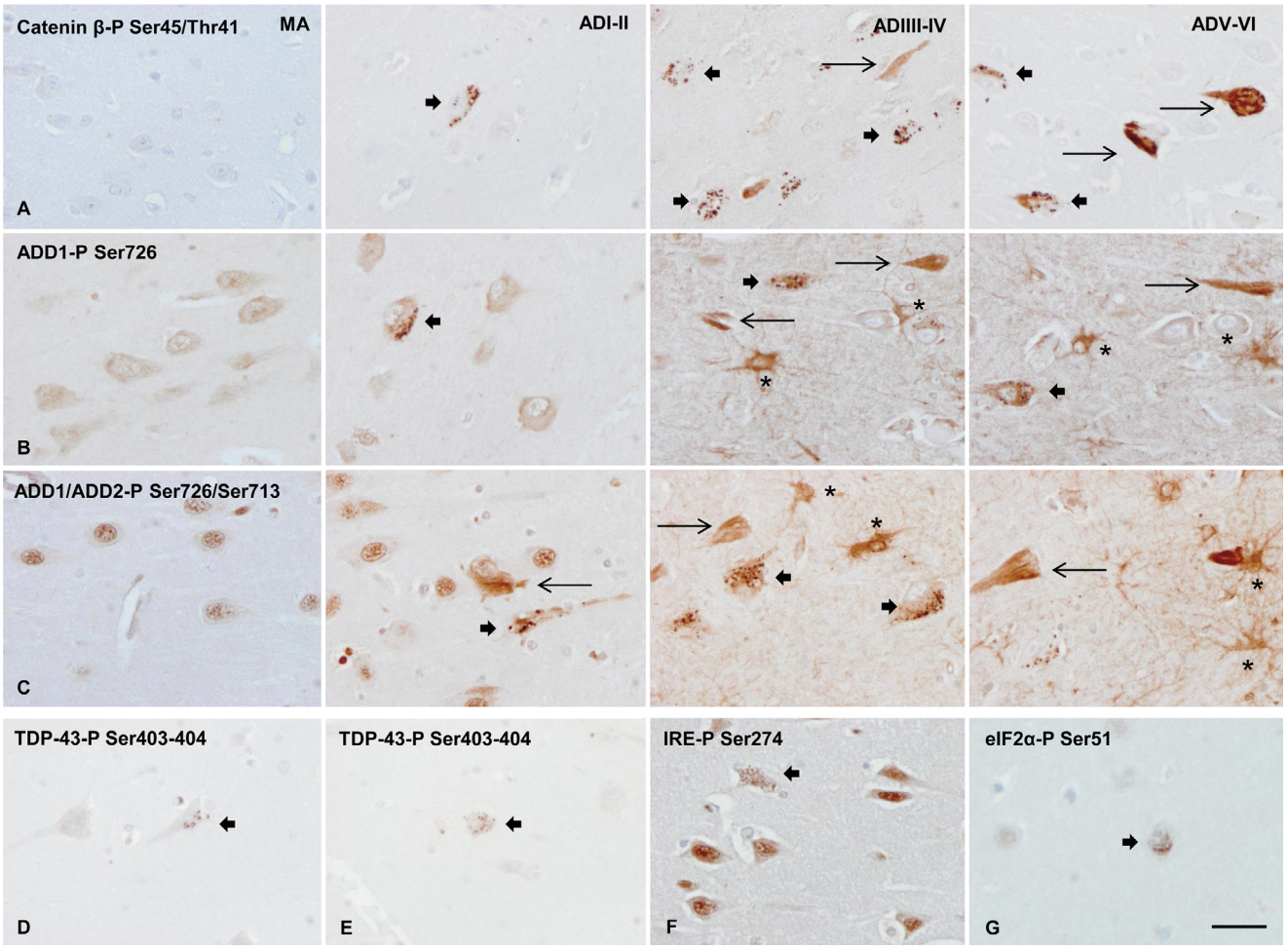

Fig. 4. Immunohistochemistry of phosphorylated proteins catenin β-P Ser45/Thr41, ADD1-P Ser726, and ADD1/ADD2-P Ser726/Ser713, in the CA1 area of the hippocampus in MA, and at stages I–II, III–IV, and V–VI of NFT pathology. **(A)** Cytoplasmic granules in a subset of neurons (thick arrows), and fibrillary cytoplasmic deposits in neurons (thin arrows) reminiscent of NFTs show strong catenin β-P immunoreactivity. **(B)** ADD1-P and **(C)** ADD1/ADD2-P immunoreactivity is found in cytoplasmic granules in a subset of neurons (thick arrows), and cytoplasmic fibrillary inclusions consistent with NFTs (thin arrows). Both antibodies also stain reactive astrocytes (asterisks). AD stages in the upper panel (catenin-β) also relate to the middle (ADD1-P) and lower (ADD1/ADD2-P) panels. **(D, E)** Cytoplasmic granules in a subset of CA1 and CA2 neurons are stained with anti-TDP-43 Ser403-404 antibodies (thick arrows) at AD stages III–IV and V–VI. **(F)** Phosphorylated inositol-requiring enzyme 1α (IRE1α-P Ser274) immunoreactivity stains cytoplasmic granules (thick arrows), often located within a vacuole, in a subset of CA1 and CA2 neurons in an ADV–VI case. **(G)** Phosphorylated eukaryotic initiation factor 2α (eIF2α-P Ser51) is rarely encountered in neurons with cytoplasmic granules (thick arrow) in an ADV–VI case. Paraffin sections, lightly counterstained with hematoxylin, bar = 50 μm.

Please cite this article in press as: Andrés-Benito P et al. Dysregulated Protein Phosphorylation as Main Contributor of Granulovacuolar Degeneration at the First Stages of Neurofibrillary Tangles Pathology. Neuroscience (2021), https://doi.org/10.1016/j.neuroscience.2021.10.023

common at advanced AD stages. NFTs, DNs, and NT were negative (Fig. 4F).

The antibody anti-phosphorylated eukaryotic initiation factor 2 (eIF2α-P Ser51) immunostained a few neurons with cytoplasmic granules in CA1 and CA2 neurons in NFT cases. NFTs, DNs, and NT were negative (Fig. 4G).

Other non-phosphorylated kinases and proteins

Antibodies against neurofilaments of 200 kDa and 160 kDa (high and medium molecular weight neurofilaments; clones RT97 and BF10, respectively) decorated neurofilaments in the neuropil and white matter, and the soma of neurons in MA and in cases with NFT pathology. NFTs showed variable RT97 and increased BF10 immunostaining. Some DNs displayed moderate to strong RT97 and BF10 immunoreactivy. GVD was negative (data not shown).

Casein kinase-δ (CK1-δ) immunoreactivity was localized in cytoplasmic granules of a subpopulation of neurons in the CA1 and CA2 subfields at first stages of NFT pathology. The number of neurons with CK1-δ-positive cytoplasmic granules increased with NFT staging progression. NFTs, DNs, and NTs were negative with anti-CSK-δ antibodies (Fig. 2E).

Cytoplasmic granules in CA1 and CA2 neurons were stained with anti-3Rtau and anti-4Rtau antibodies (Fig. 5A–D). However, the number of positive neurons was smaller than the number of neurons with CK1-δ-immunoreactive granules as revealed in parallel sections. NFTs and DNs were also immunostained with anti-3Rtau and anti-4Rtau antibodies

In contrast to anti-catenin β-P Ser45/Thr41, the catenin β antibody stained very few cytoplasmic granules in CA1 and CA2 neurons (Fig. 5E). NFTs, DNs, and NTs were negative.

In the same line, the antibody anti-TDP-43 did not stain cytoplasmic granules (data not shown), in contrast to the antibody against TDP43-P Ser403-404.

The antibody anti-p62 immunostained the cytoplasm of a subset of neurons in the hippocampus, some of them with the morphology of NFTs. Curiously, p62-immunoreactive neurons with vacuoles rarely showed p62-positive intravacuolar granules (Fig. 5F).

Ubiquitin was found in a subset of neurons with cytoplasmic vacuoles in the CA1 and CA2 subfields. However, ubiquitin granules were not seen in most neurons with vacuoles. Curiously, ubiquitin-immunoreactive granules were also located at the periphery of the external neuronal cytoplasmic

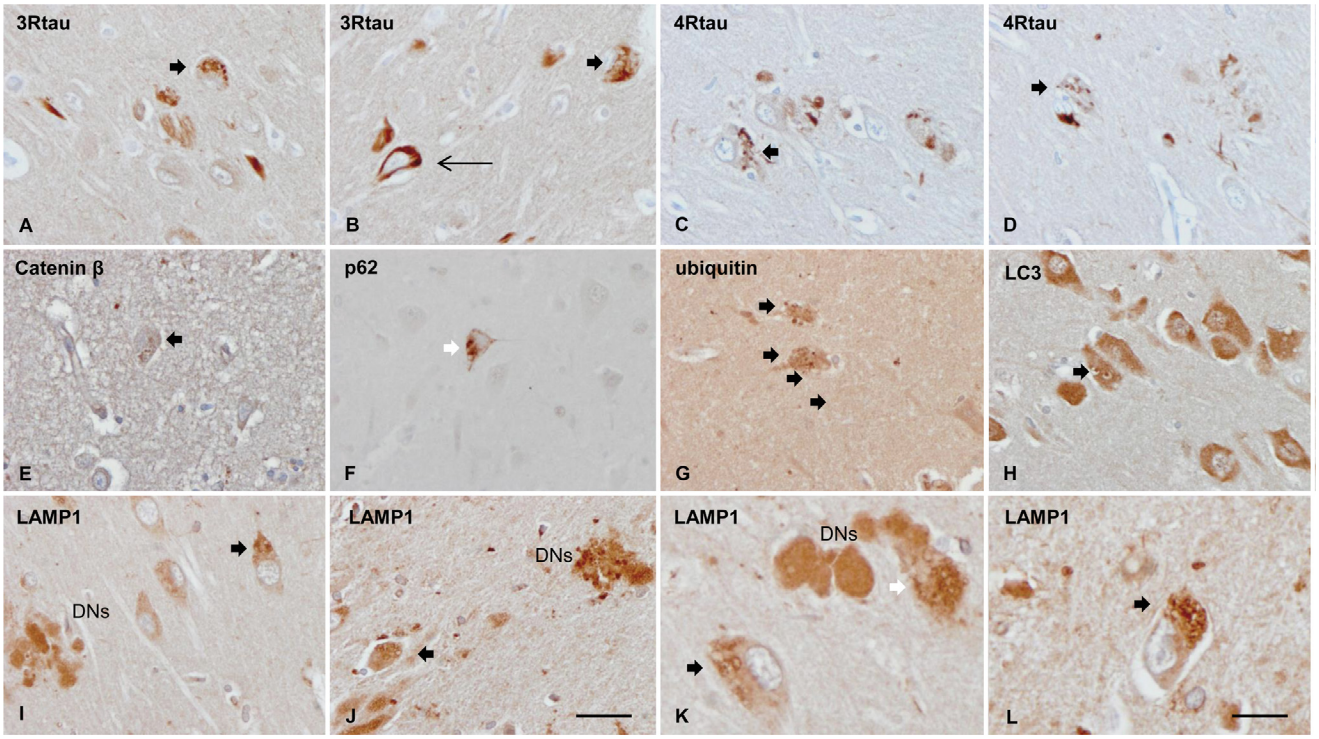

Fig. 5. **(A, B)** anti-3Rtau antibodies decorate cytoplasmic granules in a subset of CA1 neurons (thick arrows. **(C, D)** anti-4Rtau antibodies show the presence of positive cytoplasmic granules in a subset of neurons in the CA1 subfield of the hippocampus (thick arrow). NFTs are also immunostained (thin arrows). **(E)** In contrast to catenin β-P Ser45/Thr41, antibodies raised against catenin β stain a few cytoplasmic granules. **(F)** Cytoplasmic granules are rarely stained with anti-p62 antibodies, although p62 decorates the cytoplasm of neurons containing vacuoles (white arrow). **(G)** Ubiquitin immunostaining shows positive cytoplasmic granules in a few neurons; affected neurons are often accompanied by peripheral ubiquitin-positive granules. **(H)** Although uncommon, some cytoplasmic granules, often located within a vacuole, show strong LC3 immunostaining. **(I–L)** LAMP1 immunoreactivity is found in cytoplasmic vacuoles (thick arrows) and dystrophic neurites of senile plaques (DNs). A few DNs have LAMP1-positive vacuoles in addition to the diffuse granular immunostaining (white arrow). Several LAMP1-positive cytoplasmic vacuoles also contain LAMP1-immunoreactive granules inside them. Paraffin sections, lightly counterstained with hematoxylin, bar = 50 μm, excepting **(K)** and **(L)**, bar = 20 μm.

Please cite this article in press as: Andrés-Benito P et al. Dysregulated Protein Phosphorylation as Main Contributor of Granulovacuolar Degeneration at the First Stages of Neurofibrillary Tangles Pathology. Neuroscience (2021), https://doi.org/10.1016/j.neuroscience.2021.10.023

membrane (Fig. 5G). Some NFTs and most DNs contained ubiquitin; NTs were seldom positive. In short, the number of neurons with ubiquitin-positive granules was clearly smaller than the number of neurons with CK1-δ- and p38-P-immunoreactive granules as revealed in serial sections of the same cases.

Moderate LC3 immunoreactivity decorated the cytoplasm and neuronal processes. LC3 antibodies stained cytoplasmic granules in CA1 and CA2 neurons. However, the number of neurons with LC3-positive granules and the number of positive granules per cell were smaller compared with the number of neurons with CK1-δ-positive granules and the number of positive granules per neuron, when comparing serial sections of the same case. (Fig. 5H). The antibody LC3 in tissue sections does not discriminate between the cytosolic form (LC-I) and the LC3-phosphatidylethanolamine conjugate (LC3-II) which is recruited to autophagosomal membranes (Tanida et al., 2008).

Cytoplasmic vacuoles with granules in neurons of the CA1 and CA2 subfields were stained with anti-LAMP1. LAMP1 antibodies also decorated DNs with a diffuse pattern, but very rarely NFTs; NTs were negative, as detailed elsewhere (Barrachina et al., 2006). LAMP1 immunoreactivity was observed inside the vacuoles in a subpopulation of neurons. LAMP1-positive vacuoles were distinguished in some DNs in addition to the diffuse immunostaining (Fig. 5I–L).

Table 1 summarizes the immunohistochemical characteristics of GVD, NFT, SPs and NTs in the CA1 region of the hippocampus in cases with NFT pathology stages V–VI.

Double-labeling immunofluorescence and confocal microscopy

Double-labeling immunofluorescence was carried out in selected tissue sections to elucidate the relationship between p38-P, SAPK/JNK-P, GSK3 α/β-P, PK1-P, and SRC-P, and phospho-tau deposits, as revealed with the antibodies AT8 and P-tauThr181.

p38-P-positive cytoplasmic granules were not stained with the antibody AT8. p38-P immunoreactivity was observed in a few neurons with variable amounts of P-

Table 1. Localization of kinases and selected phosphorylated and non-phosphorylated proteins in the CA1 subfield of the hippocampus in cases with NFT pathology; GVD: granulovacuolar degeneration; NFTs: neurofibrillary tangles; DN/SPs: dystrophic neurites of senile plaques; NPs: neuropil threads. Semi-quantitative assessment of lesions in the CA1 region of ADV–VI cases detailed in methods; values for GVD, + + +: 20–30% of total neurons; + +: 10–19; +: 1–9%; +/–: not present in all sections; values for NFT, ###: 50–70%; ##: 20–49%; #: 1–19%; #/–: not present in all sections. The evaluation of immunoreactivty in dystrophic neurites of senile plaques and neuropil threads expressed as §§§, §§, §, – indicate abundant, moderate number, rarely stained or not stained at all, respectively

	granules/GVD	NFTs	DN/SPs	NTs	others
p38-P Thr180/Tyr182	+ + +	#	§	–	
SAPK/JNK-P Thr183/Thr185	+	##	§§§	§	
PKA α/β-P Thr197	+ +	#	–	–	
SRC-P Tyr416	+, ↓	#, =, ↓	–	–	
GSK 3α/β-P Tyr279/Tyr216	+ +	#/–	–	–	
GSK 3 β Ser9	–	##	§§	–	
PAK1-P Ser199/Ser204	+ +	##	–	–	
CAMK2A-P Tyr786	+ +	–	–	–	
PKCG-P Thr655	+ +	–	–	–	
CK1-δ	+ + +	–	§§	–	
3Rtau	+	##	§§	§	
4Rtau	+	##	§§	§	
Tau AT8	–	###	§§§	§§§	
Tau-P Thr181	–	###	§§§	§§§	
Tau-P Ser262	+ +	###	§§§	§	
MAP2-P Thr1620/1623	+	###	§§§	§§	
MAP1B-P Thr1265	+	–	–	–	
NFL-P Ser473	–	#/–	§/–	–	
NFH (200 kDa) RT97	–	#/–	§/–	–	
NFM (160 kDa) BF10	–	#/–	§/–	–	
ADD1-P Ser726	+	#	–	–	astrocytes
ADD/1/ADD2-P Ser726/Ser713	+	#	–	–	astrocytes
catenin β	+/–	–	–	–	
catenin β-P Ser45/Thr41	+ +	#	–	–	
TDP-43	–	–	–	–	
TDP-43-P Ser409	+	–	–	–	
IRE-P Ser 274	+	–	–	–	
eIF2α-P Ser51	+	–	–	–	
p62	+	#	§	–	
ubiquitin	+	#	§§	§	
LC3	+	–	–	–	
LAMP1	+ +	–	§§§		microglia

Please cite this article in press as: Andrés-Benito P et al. Dysregulated Protein Phosphorylation as Main Contributor of Granulovacuolar Degeneration at the First Stages of Neurofibrillary Tangles Pathology. Neuroscience (2021), https://doi.org/10.1016/j.neuroscience.2021.10.023

tau deposition in the cytoplasm, some of them considered pre-tangles (Fig. 6A, B). NFTs were rarely stained with anti-p38-P antibodies while some neurons contained p38-P-immunoreactive granules with no trace of AT8 immunoreactivity (Fig. 6C).

SAPK/JNK-P immunoreactivity decorated cytoplasmic granules in neurons, but not in AT8-positive neurons (data not shown). Neurons with pre-tangles showing AT8 perinuclear immunoreactivity were negative with anti-SAPK/JNK-P antibodies (Fig. 6D). In contrast, strong SAPK/JNK-P immunoreactivity co-localized with AT8-tau in NFTs (Fig. 6E).

GSK3 α/β-P immunoreactivity decorated the cytoplasmic granules in a few neurons in the CA1 and CA2 areas of the hippocampus that did not contain tau-P Thr181 in the cytoplasm. Neurons with NFTs and without NFTs were weakly immunostained with anti-GSK3 α/β-P antibodies (Fig. 7A).

Anti-PAK1-P antibodies decorated cytoplasmic granules in a subset of neurons in the CA1 and CA2 subfields. The cytoplasmic granules were negative with AT8, but AT8 immunoreactivity was present in the cytoplasm of neurons containing PAK1-P-positive granules; AT8 deposits in these neurons had the morphology of pre-tangles (Fig. 7B). In contrast, NFTs rarely displayed PK1-P immunoreactivity (Fig. 7C).

The intensity of SRC-P immunoreactivity varied in individual neurons in cases with NFTs. SRC-P immunoreactivity increased in some neurons without tau-P Thr181 deposits, but SRC-P immunoreactivity was reduced in most neurons with NFTs. Neurons with increased SRC-P and tau-P THr181 deposits were seldom observed (Fig. 7D, E).

MAP2-P immunoreactivity showed the same pattern of NFT immunostaining as the antibody AT8. NFTs were strongly stained with anti-MAP2-P antibodies; neurons without NFTs were not (Fig. 8A, B). In contrast, moderate ADD1-P immunoreactivity was seen in the cytoplasm of neurons in MA and cases with NFT pathology. Increased ADD1-P immunoreactivity occurred in the cytoplasmic granules in a subset of neurons. Although granules were negative with AT8, most neurons with ADD1-P-immunoreactive granules showed cytoplasmic AT8 immunoreactivity (Fig. 8C, D). NFTs were rarely stained with anti-ADD1-P antibodies (Fig. 8D).

In order to learn about the relationship between CK1-δ and other cytoplasmic granule markers double-labelling immunofluorescence was assessed in selected tissue sections. LC3-positive granules were scanty and rarely co-localized with the most abundant CK1-δ-immunoreactive granules (Fig. 8E).

In contrast, CK1-δ-positive granules commonly co-localized with p38-P, MAP1B-P, CAMK2A-P, PKA α/β-P, and tau-P Ser262 (Fig. 9). This does not mean complete co-localization, as a minority of CK1-δ-positive granules were not stained with anti-p38-P or with anti-CAMK2A-P antibodies (Fig. 9A and C), and a few MAP1B-P- and PKA α/β-P-immunoreactive granules were not stained with anti-CK1-δ antibodies (Fig. 9B and D). In contrast to tau AT8 and tau-P Thr181, tau-P Ser262 co-localized with CK1-δ in the cytoplasmic granules (Fig. 9E).

Double-labelling with LAMP1 and CK1-δ showed variable co-localization. Some neurons, particularly at first stages of NFT pathology showed CK1-δ-positive cytoplasmic granules without surrounding vacuoles. However, increased LAMP1 immunoreactivity was diffuse in the cytoplasm (Fig. 10A). Other neurons contained CK1-δ-immunoractive granules with no vacuoles and no increase in LAMP1 immunoreactivity. Mature GVD was characterized by CK1-δ-positive granules inside LAMP1-immunoreactive vacuoles. Yet not all granules were surrounded by LAMP1-immunoreactive membranes, thus suggesting free localization of a relatively percentage of CK1-δ-positive granules in neurons at advanced stages of NFT pathology with mature GVD (Fig. 10B, C).

DISCUSSION

Cytoplasmic granules in CA1 neurons are common in cases with NFT pathology, and their number, although with individual variations, increases with NFT stage progression. Cytoplasmic granules are better visualized with selected antibodies than in haematoxylin and eosin-stained sections. Some of them lack a surrounding membrane and do not appear as classical GVDs. This is probably due in part to the different pathways that cytoplasmic granules follow in neurons; some of them are recruited in NFTs; others will form the core of GVDs. It is difficult to ascertain the eventual fate of a particular cytoplasmic granule at the time in which it lacks a membrane. Moreover, GVD can be found in neurons with tangles; instead, neurons with tangles usually lack vacuoles with granules inside in most brain regions, including the hippocampus. That means that GVD and NFTs are distinct neuronal alterations. Commonalities and differences are detailed below.

Kinases and other proteins in GVD

Various kinases are localized in neurons with GVD. Some of them identify the granules with antibodies directed to

Fig. 6. Double-labeling immunofluorescence and confocal microscopy of p38-P Thr180/Tyr182 (green) and AT8 (tau-P Ser202/Thr205; red) **(A–C)**, and SAPK/JNK-P (green) and AT8 (red) **(D, E)** in the hippocampus at stages III–IV of NFT pathology. p38-P is found in small granules in the cytoplasm of neurons with weak or moderate phospho-tau deposits (long arrowheads) and early phospho-tau deposits **(A, B)**. Some neurons have only p38-P-immunoreactive granules with no phospho-tau (thick arrows), and others only phospho-tau without p38-P-positive granules (thin arrows) **(C)**. SAPK/JNK-P immunoreactivity is not seen in neurons with pre-tangles **(D)**. In contrast, strong SAPK/JNK-P immunoreactivity co-localizes with phospho-tau in NFTs **(E)**. Nuclei are labeled with DRAQ5™ (blue). Paraffin sections, bar = 20 μm. (For interpretation of the references to colour in this figure legend, the reader is referred to the web version of this article.)

Please cite this article in press as: Andrés-Benito P et al. Dysregulated Protein Phosphorylation as Main Contributor of Granulovacuolar Degeneration at the First Stages of Neurofibrillary Tangles Pathology. Neuroscience (2021), https://doi.org/10.1016/j.neuroscience.2021.10.023

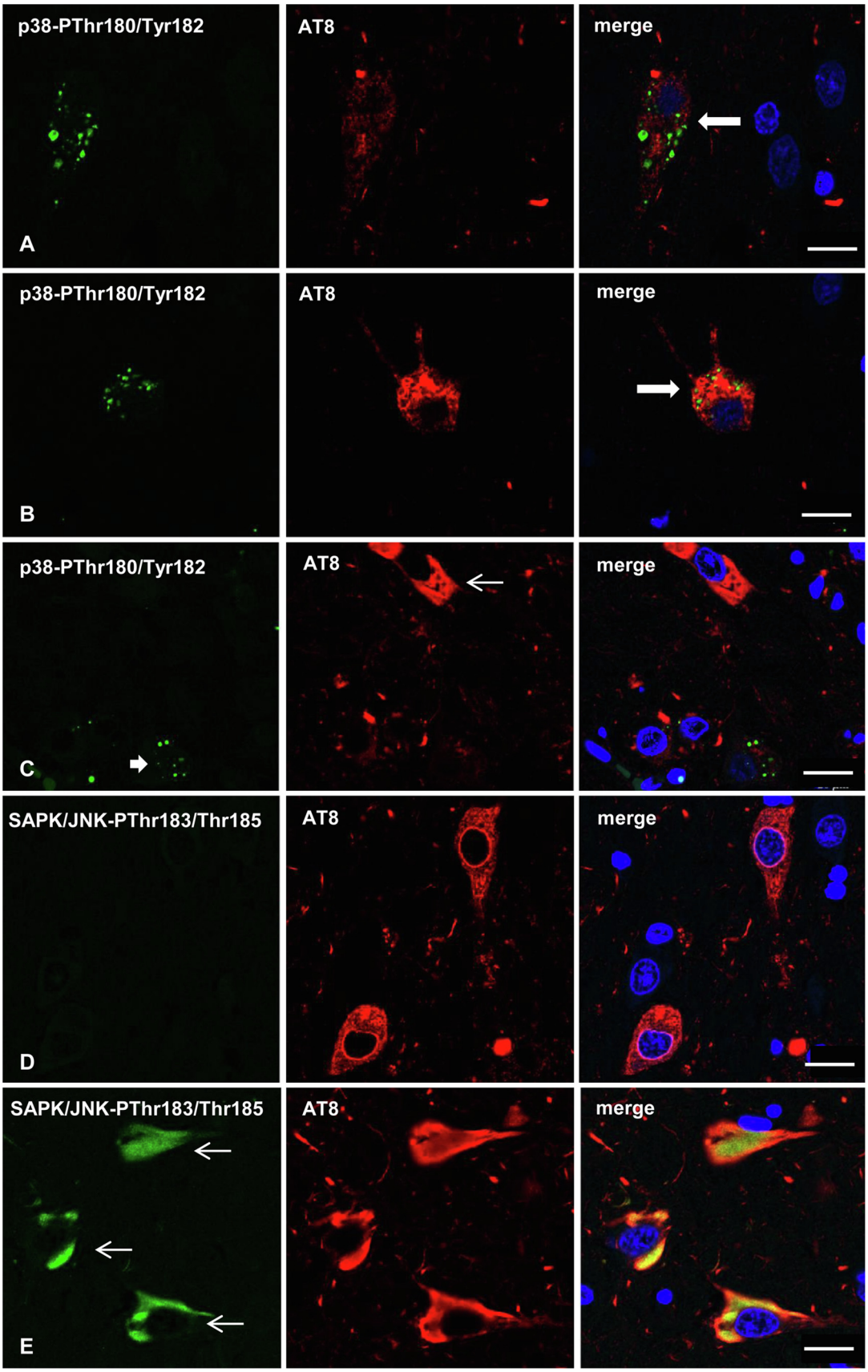

Please cite this article in press as: Andrés-Benito P et al. Dysregulated Protein Phosphorylation as Main Contributor of Granulovacuolar Degeneration at the First Stages of Neurofibrillary Tangles Pathology. Neuroscience (2021), https://doi.org/10.1016/j.neuroscience.2021.10.023

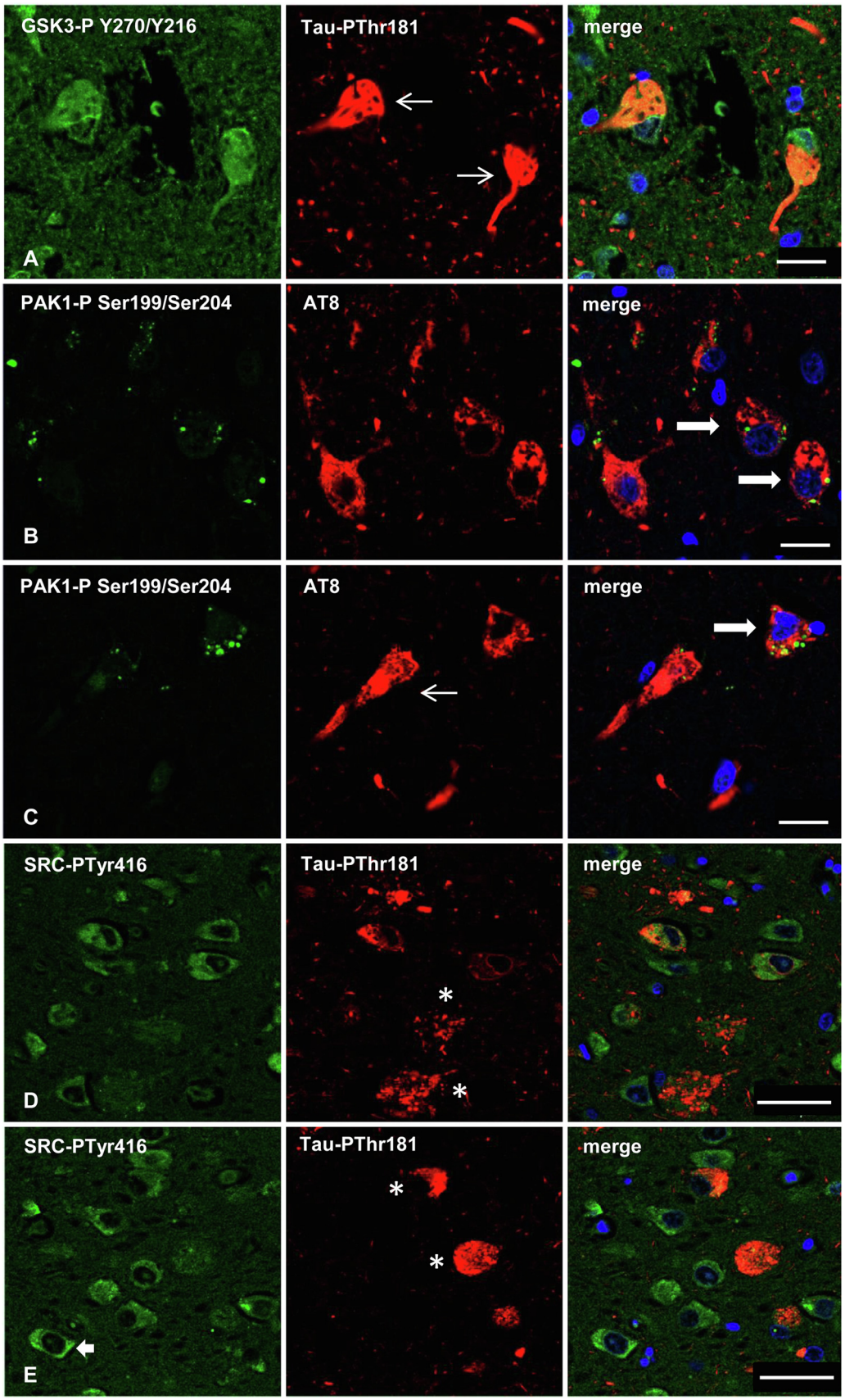

Please cite this article in press as: Andrés-Benito P et al. Dysregulated Protein Phosphorylation as Main Contributor of Granulovacuolar Degeneration at the First Stages of Neurofibrillary Tangles Pathology. Neuroscience (2021), https://doi.org/10.1016/j.neuroscience.2021.10.023

non-phospho-specific epitopes of the proteins, such as casein kinase 1 isoforms (CK1-α, δ, and ε) (Ghoshal et al., 1999; Schwab et al., 2000; Kannanayakal et al., 2006), cyclin-dependent kinase-5 (cdk5) (Nakamori et al., 2012), dual-specificity tyrosine-phosphorylation-regulated kinase 1 A (DYRK1A) (Wegiel et al., 2008), and SRC tyrosine kinase (SRC) (Bhaskar et al., 2005). Other kinases are detected in the granules using phospho-specific antibodies. Active glycogen synthase kinase 3β (P-GSK-3α and GSK-3β) (Leroy et al., 2002), p38-activated mitogen-activated protein kinase (p38-P) (Zhu et al., 2000), stress-activated protein kinase/c-Jun N-terminal kinase (SAPK/JNK-P) (Lagalwar et al., 2007), and active p70 S6 kinase (An et al., 2003) are among this group.

Our results confirm the presence of CK1-δ, p38-P Thr180/Tyr182 (p38-P), stress-activated protein kinase/c-Jun N-terminal kinase Thr183/Thr185 (SAPK/JNK-P), glycogen synthase kinase 3α/β Tyr279/Tyr216 (GSK-3α/β-P), and GSK-3β Ser9 in the cytoplasmic granules in a subset of neurons of the CA1 and CA2 areas of the hippocampus. Also, we identify for the first time the presence of phosphorylated protein kinase A or cyclic AMP-dependent protein kinase A Thr197 (PKA α/β-P), SRC tyrosine kinase Tyr 416 (SRC-P), serine threonine protein kinase 1 Ser199/Ser204 (PAK1-P), calcium-calmodulin kinase 2A Tyr197 (CAMK2A-P), and protein kinase C type γ Thr655 (PKCG-P) in cytoplasmic granules in a subset of neurons in the CA1 and CA2 subfields in cases with NFT pathology, but not in MA cases.

Previous studies identified several proteins in the cytoplasmic granules in subsets of CA1 and CA2 neurons: cleaved amyloid protein, phospho-catenin-β, cleaved caspase 3, charged multivesicular body protein 2B, phospho-c-Jun, phosphorylated eukaryotic initiation factors, phosphorylated inositol-requiring enzyme 1α (IREα), phosphorylated mammalian target of rapamycin (mTOR), ribosomal proteins, Smads 2 and 3, p62, and ubiquitin among others (Okamoto et al., 1991; Love et al., 1988; Stadelmann et al., 1999; Selznick et al., 1999; Su et al., 2002; Ghanevati and Miller, 2005; Lee et al., 2006; Ueberham et al., 2006; Thakur et al., 2007; Chalmers and Love, 2007; Hoozemans et al., 2009; Castellani et al., 2011; Funk et al., 2011; Köhler, 2016). Our results confirm the presence of phospho-β-catenin Ser45/Thr41 (but also the low expression of catenin-β), IREα-P Ser274, eIF2α-P Ser51, TDP-43-P Ser403-404 (but absent TDP-43), and ubiquitin. We have identified other phosphorylated proteins in the cytoplasmic granules such as MAP2-P Thr1620/1623, MAP1B-P Thr1265, ADD1-P Ser726, and ADD1/ADD1-P Ser726/Ser713.

Common and differential composition of GVD, and NFTs, DNs and NTs

Several phosphorylated kinases are expressed in subsets of neurons with pre-tangles and NFTs (Arendt et al., 1995; Perry et al., 1999; Hensley et al., 1999; Pei et al., 1999; Zhu et al., 2000; Zhu et al., 2001a,b; Zhu et al., 2002; Pei et al., 2001; Atzori et al., 2001; Ferrer et al., 2001a,b; Pei et al., 2002a,b; Ferrer et al., 2002; Sun et al., 2003; Ferrer, 2004; Ferrer et al., 2005). The expression of such active kinases is accompanied by the activation of the corresponding upstream activators in neurons with NFTs (Arendt et al., 1995; Ferrer et al., 2001a,b; Zhu et al., 2001c, Pei et al., 2002a,b; Zhu et al., 2003a, Zhu et al., 2003b). The present study confirms the existence of p38-P Thr180/Tyr182, SAPK/JNK-P Thr183/Thr185, GSK 3α/β-P Tyr279/Tyr216, and GSK3β-P Ser9 in neurons with pre-tangles and tangles. p38-P immunoreactivity appears at early stages of tau deposition, whereas SAPK/JNK-P, and the active and inactive forms of GSK-3α/β-P, appear at more advanced stages. Particularly, pre-tangles bearing typical hyperphosphorylated perinuclear deposition are not stained with anti-SAPK/JNK-P antibodies in our series. Mature NFTs show strong SAPK/JNK-P immunoreactivity. Other kinases also associate with NFTs. Some of them are identified with antibodies not directed to active forms like cell division cycle (cdc2), cdk5, CK1-δ, GSK-3β, and microtubule-affinity regulating kinase (MARK) (Liu et al., 1995; Yamaguchi et al., 1996; Pei et al., 1997; Pei et al., 1998; Schwab et al., 2000; Chin et al., 2000; Borghi et al., 2002). Other kinases are recognized with antibodies directed against the active (phosphorylated) forms being cdc2-P (Vincent et al., 1997; Pei et al., 2002a,b), protein kinase B (PKB-P) (Pei et al., 2003), and p70 S6 kinase (An et al., 2003).

Our study identifies new kinases in NFTs. PKA α/β-P Thr197 and PAK1-P Ser199/Ser204 antibodies decorate subsets of pre-tangles and NFTs. Double-labelling immunofluorescence with anti-SRC-P and anti-P-tau-Thr181 reveals a curious scenario; many neurons with pre-tangles and NFTs show reduced SRC-P immunoreactivity, while increased SRC-P immunoreactivity is mainly found in neurons without P-tau Thr181deposits. Since different phospho-tau epitopes may be expressed in neurons (Köhler, 2016), this observation does not necessarily indicate an opposing relation between phospho-tau and SRC-P in selected

Fig. 7. Double-labeling immunofluorescence and confocal microscopy of GSK3 αβ-P Tyr279/Tyr216 (green) and tauP-Thr181 (red), PAK1-P Ser199/Ser204 (green) and AT8 (red) **(B, C)**, and SRC-P Tyr 416 (green) and tauP-Thr181 (red) **(D, E)** in the hippocampus at stages III–IV of NFT pathology. GSK3 αβ-P is found in neurons with phosphorylated tau deposits (**(A)**, thin arrows). Anti-PK1-P antibodies stain cytoplasmic granules in a subset of neurons. The cytoplasmic granules are negative with the AT8 antibody, but AT8 immunoreactivity is found in the cytoplasm of neurons with pre-tangles containing PK1-P-positive granules (**(B)**, thick large arrows); however, PK1-P immunostaining is very rare in NFTs (C, thin arrows). The intensity of SRC-P immunostaining is increased in some neurons without P-tau deposits (thick arrow), but it is reduced in the majority of neurons with NFTs (asterisks) **(D, E)**. Nuclei are labeled with DRAQ5™ (blue). Paraffin sections, **(A–C)**, bar = 20 μm; **(D, E)**, bar = 40 μm. (For interpretation of the references to colour in this figure legend, the reader is referred to the web version of this article.)

Please cite this article in press as: Andrés-Benito P et al. Dysregulated Protein Phosphorylation as Main Contributor of Granulovacuolar Degeneration at the First Stages of Neurofibrillary Tangles Pathology. Neuroscience (2021), https://doi.org/10.1016/j.neuroscience.2021.10.023

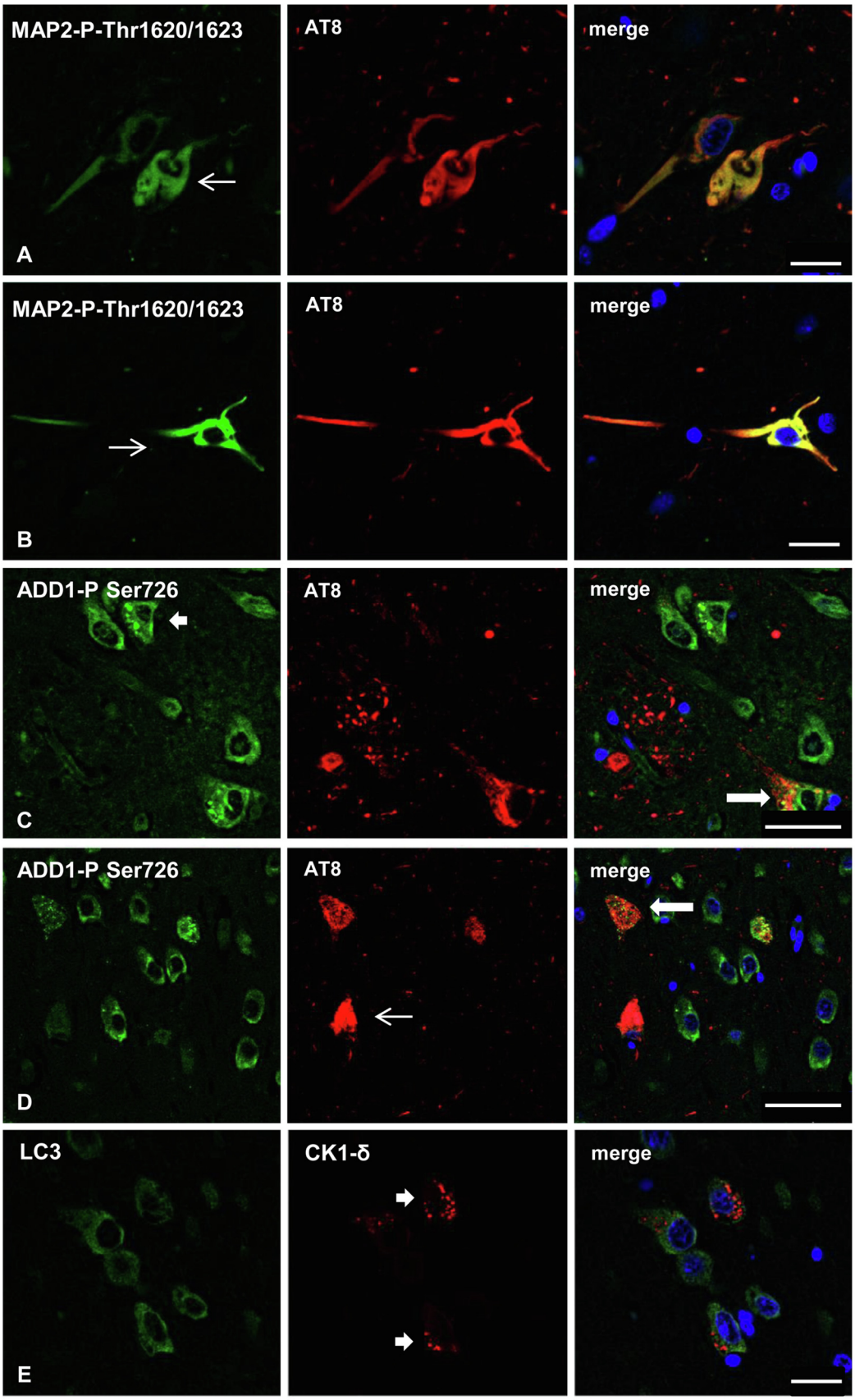

Please cite this article in press as: Andrés-Benito P et al. Dysregulated Protein Phosphorylation as Main Contributor of Granulovacuolar Degeneration at the First Stages of Neurofibrillary Tangles Pathology. Neuroscience (2021), https://doi.org/10.1016/j.neuroscience.2021.10.023

neurons, but rather an opposite correlation between SRC-P and this particular anti-P-tau epitope.

In contrast to NFTs and cytoplasmic granules, a limited number of active kinases are localized in dystrophic neurites of SPs: SAPK/JNK-P, GSK-3α/β-P, and p38-P. Neuropil threads are not stained, with the assessed anti-kinase antibodies used in the present study excepting for SAPK/JNK-P.

P38-P is more abundant in GVD than in NFTs, but the opposite occurs regarding SAPK/JNK-P. GSK 3α/β-P Tyr279/Tyr216 predominates in cytoplasmic granules but GSK 3 β Ser9 in NFTs. CAMK2A-P and PKCG-P, and CK1δ only localize in granular cytoplasmic inclusions but not in NFTs.

One of the main differences between GVD and NFT is the participation of different tau species. A summary of principal phospho-tau species in NFTs is detailed elsewhere (Ferrer et al., 2014). Several phospho-tau species in NFTs are absent in GVD excepting Ser-P Ser262, among a few others (Köhler, 2016). In contrast, antibodies directed to several tau species truncated at the N-terminal recognize components of GVD (Bondareff et al., 1991; Dickson et al., 1993; Leroy et al., 2002).

Regarding other proteins, NFTs are enriched in MAP2-P Thr1620/1623, while MAP1B-P Thr1265 is restricted to GVD; NFLs are absent in GVD but present in NFTs. Phosphorylated TDP-43-P is present in the granules of GVD, as already reported (Kadokura et al., 2009), but not in NFTs.

Immunohistochemistry to CK1-α and AT8, and laser microdissection have identified the proteomes of neurons containing GVD and NFTs, respectively, using label free LC-MS/MS (Hondius et al., 2021). A significant change in abundance of 115 proteins in GVD-containing neurons and 197 in NFT-containing neurons was observed compared to control neurons (Hondius et al., 2021). The method used in that survey did not permit the identification of phosphorylated proteins. The added value of our investigation is the identification of several new phosphorylated kinases and phosphorylated proteins in GVD which are differentially expressed when compared with NFTs and DNs. Commonalities and differences between GVD, NFTs, DNs and NTs are summarized in Table 1.

Variability of GVD, and convergence of pathogenic pathways

Some neurons show typical vacuoles with dense inclusions characteristic of GVD in which the granules are immunostained with most of the antibodies assessed in the present study. However, the number of positive granules is variable depending on the antibody thus proving that not all the phosphorylated and non-phosphorylated components are present in every neuron with GVD. This is not new, as the variability of integrants in GVDs including tubulins, neurofilaments, phospho-tau species, p62, and ubiquitin has been detailed (Köhler, 2016). Casein kinase 1α (CK1-α) isoforms and charged multivesicular body protein 2B (CHMP2B) are considered good markers of GVD (Ghoshal et al., 1999; Schwab et al., 2000; Funk et al., 2011). However, the number of neurons with CHMP2B-immunoreactive granules is higher than the number of neurons with GVD (Yamazaki et al., 2010). Table 1 further illustrates the variable incidence of the different components in the present series.

Some granules in neurons with GVD co-localize with markers of the unfolded protein response (UPR) in neurons with pre-tangles, including phosphorylated PKR-like ER kinase (PERK-P), IRE1-α-P, and phosphorylated eukaryotic translation initiation factor 2α (eIF2-α-P) (Hoozemans et al., 2005; Hoozemans et al., 2009). Markers of the UPR are also observed in neurons with NFTs (Unterberger et al., 2006), and in neurons with no evidence of pre-tangle stage in the present series. However, the number of neurons with eIF2α-P Ser51-immunoredactive granules is lower than the number of neurons with IRE-P Ser 274-immunoractive granules. Furthermore, the number of neurons with CK1-δ- or p38-P-positive granules roughly doubles the number of neurons with IRE-P Ser 274-positive granules.

GVD bodies contain LC3 and p62, while others are surrounded by LAMP1 immunoreactivity, thus suggesting progression to late-stage autophagic vacuoles (Funk et al., 2011). However, LC3 is not a constant component of GVD, and p62 is very rare. p62 and ubiquitin also recognize a subset of NFTs and DNs in sAD. LAMP1 is associated with later stages of autophagy. LAMP1 immunoreactivity in neurons containing cytoplasmic granules is often manifested as fine granular imunoreactivity in the cytoplasm with occasional ring-like condensation consistent with the membrane of the vacuole (Funk et al., 2011). However, not all cytoplasmic granules stained with p38-P and CK1-δ are localized within a vacuole, or at least they are not surrounded by a LAMP1-immunoreactive membrane.

The molecular composition of cytoplasmic granules suggests a convergence of altered proteolysis, impaired ubiquitin–proteasome system, abnormal reticulum stress responses, and altered endocytic and autophagic

Fig. 8. Double-labeling immunofluorescence and confocal microscopy of MAP2-P Thr1620/1623 (green) and AT8 (red) **(A, B)**, ADD1-P Ser726 (green) and AT8 (red) **(C, D)** in the hippocampus at stages III–IV of NFT pathology. MAP2-P is co-localized with AT8 in NFTs **(A, B)**. Increased ADD1-P immunoreactivity occurs in cytoplasmic granules inside vacuoles in neurons without AT8-immunoractive deposits (**(C)**, short thick arrow), neurons with AT8-immunoreactivity in the cytoplasm outside of vacuoles (**(C, D)**, long thick arrow). However, NFTs are usually not stained with anti-ADD1-P antibodies (**(D)**, thin arrow). Representative image of double-labeling immunofluorescence with LC3 and CK1-δ antibodies shows LC3 negativity in CK1-δ-positive granules (white short arrows). Nuclei are labeled with DRAQ5™ (blue). Paraffin sections, **(A, B, F)**, bar = 20 μm; **(C)**, bar = 30 μm; **(D)**, bar = 50 μm. (For interpretation of the references to colour in this figure legend, the reader is referred to the web version of this article.)

Please cite this article in press as: Andrés-Benito P et al. Dysregulated Protein Phosphorylation as Main Contributor of Granulovacuolar Degeneration at the First Stages of Neurofibrillary Tangles Pathology. Neuroscience (2021), https://doi.org/10.1016/j.neuroscience.2021.10.023

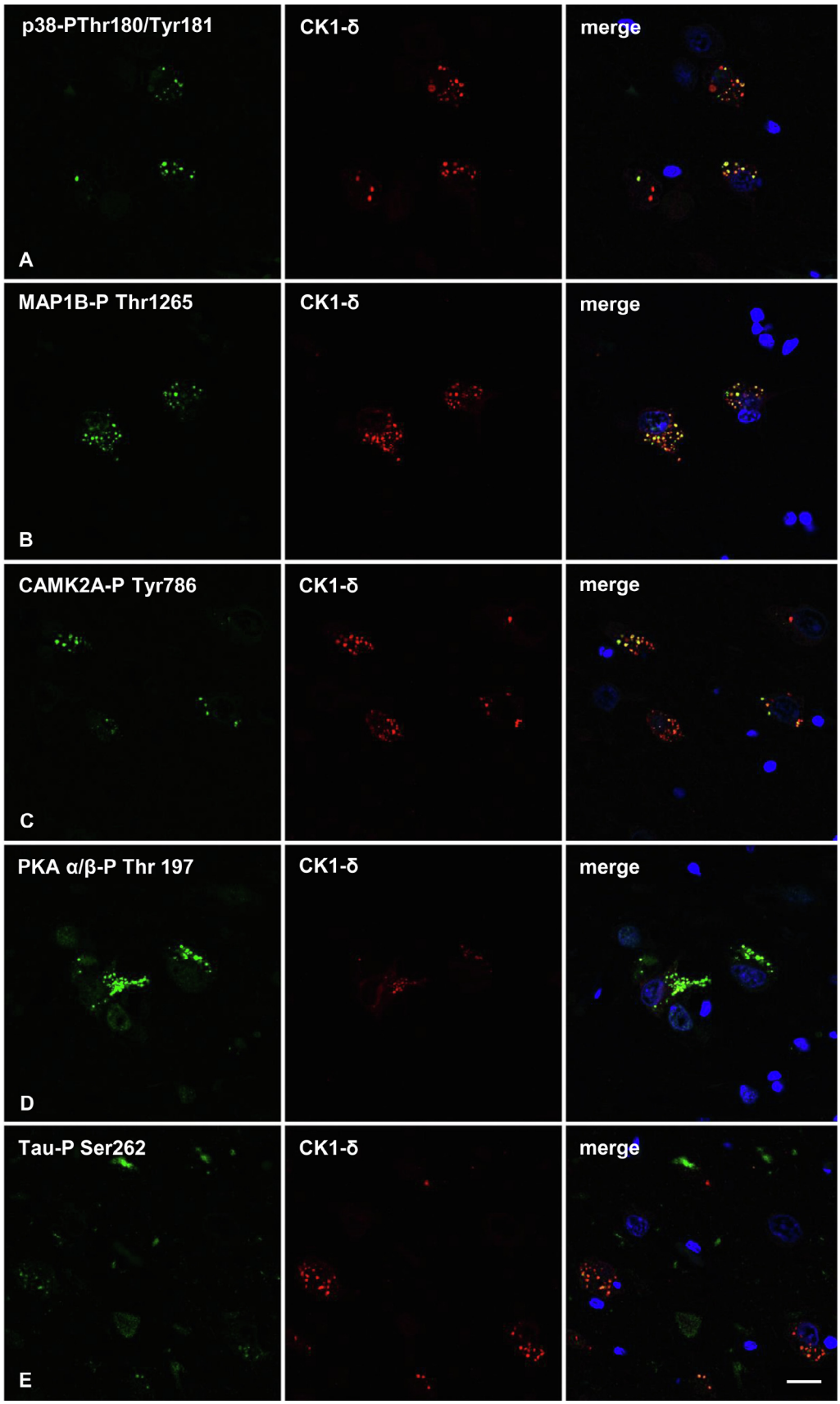
p38-PThr180/Tyr181
CK1-δ
merge
A
MAP1B-P Thr1265
CK1-δ
merge
B
CAMK2A-P Tyr786
CK1-δ
merge
C
PKA α/β-P Thr 197
CK1-δ
merge
D
Tau-P Ser262
CK1-δ
merge
E

pathways (Okamoto et al. 1991; Oyanagi and Ikuta, 1974; Krigman et al., 1965; Aberle et al., 1997; Ghanevati and Miller, 2005; Hoozemans et al., 2005; Barrachina et al., 2006; Hoozemans et al., 2009; Funk et al., 2011; Funk and Kuret, 2012). Recently, mitophagy was added to the list of alterations linked to GVD (Hou et al., 2020). However, early stages of GVD contain only granules and not vacuoles.

It is suggested that tau is the main candidate for triggering GVD (Köhler, 2016). GVD is the first cellular response that develops before the appearance of pre-tangles. Later on, the number of tangles increases in parallel to the decrease in the number of GVDs (Hoozemans et al., 2009; Yamazaki et al., 2011; Nijholt et al., 2012; Köhler, 2016). Tau pathology provokes the generation of GVDs in different mouse models *in vivo* and in primary neurons *in vitro* (Ishizawa et al., 2003; Köhler et al., 2013; Köhler et al., 2014; Wiersma et al., 2019; Wiersma and Scheper, 2020). In short, the most widely accepted model follows the scheme: abnormal tau in pretangles induces abnormal reticulum stress responses, which in turn trigger endocytic and autophagic pathways in the face of impaired proteolysis and UPS function. This scenario is consistent with the idea that GVD is the final stage of an active process linked to failed degradation of abnormal protein aggregates in the cytoplasm of a subpopulation of neurons.

Early kinase activation and abnormal phosphorylation as key factors in the pathogenesis of GVD

Although GVD can be induced by tau pathology in particular settings (Wiersma et al., 2019), it is not clear that tau is the only inducer of GVD in AD. Several proteomics and network analysis in cellular and animal models have shown a large number of tau interactors and modulators; interacting proteins include microtubule-associated proteins, synaptic proteins, membrane proteins, major protein complexes involved in RNA processing and translation, several heat shock proteins, the proteasome, and kinases and phosphatases, among many others (Gunawardana et al., 2015; Stancu et al., 2019; Sinsky et al., 2020; Feuillette et al. 2020). Recent quantitative proteomics on micro-dissected NFTs and affinity purification-mass spectrometry used to pinpoint which of the identified proteins specifically binds to phosphorylated tau, reveal that 75 proteins in NFTs interact with phospho-tau (Drummond et al., 2020). Several components of NFTs do not interact with phospho-tau, thereby indicating that NFTs are not composed only of phospho-tau and phospho-tau interactors.

A similar scenario is suggested here for GVD. Our study identifies several proteins, and particularly phosphorylated kinases as new components of cytoplasmic granules. Phosphorylation is one of the most common and essential mechanisms of protein function. This posttranslational modification mostly results from activation/inhibition of protein function and/or recruitment of interacting proteins with structurally conserved domains. Most identified phosphorylated kinases are active forms which phosphorylate various substrates including tau. Other kinases are not tau kinases. Most identified active kinases and phosphorylated proteins are found in the cytoplasmic granules before the appearance of pre-tangles and tangles in the CA1 and CA2 subfields of the hippocampus; most of them appear before the appearance of LAMP1-positive vacuoles. Among kinases, p38-P, SAPK/JNK-P, MAPK/ERK-P, PKA α/β-P, SRC-P, GSK3β-P, PAK1-P, CAMK2A-P, PKCG-P, and CK1-δ are identified in the cytoplasmic granules at stages I–II of NFT pathology. Also, the cytoplasmic granules in neurons contain tau-P Ser262, MAP1B-P, ADD1-P, ADD1/ADD2-P, catenin β-P, and TDP-43-P at stages I–II of NFT pathology. In contrast, 3Rtau and 4Rtau in granules are not as common as tau-P Ser262; non-phosphorylated catenin β is scanty, and non-phosphorylated TDP-43 is absent in granules when compared with the corresponding phosphorylated forms. These findings support the idea that abnormal hyperphosphorylation driven by diverse active kinases is an early event in the pathogenesis of GVD. Exacerbated activated kinases phosphorylate different substrates including some tau species, among other proteins. Markers of the UPS, reticulum stress response and autophagy appear later. In summary, the present findings point to early phosphorylation of kinases leading to their activation, and resulting in the abnormal phosphorylation of various substrates, including tau, as a principal inducer of GVD.

FUNDING

The project leading to these results has received funding from "La Caixa" Banking Foundation under the project HR18-00452 to IF; it was also supported by the Ministry of Economy and Competitiveness, Institute of Health Carlos III (ISCIII) (co-funded by European Regional Development Fund, ERDF, a way to build Europe): FISPI17/000809 to IF; and the Intra-CIBERNED 2019 collaborative project to IF and JADR. We thank CERCA Programme/Generalitat de Catalunya for institutional support.

Fig. 9. Double-labeling immunofluorescence and confocal microscopy of CK1-δ (green) and p38-P, MAP1B-P, CAMK2A-P, PKA α/β-P and tau-P Ser262 (red) in the hippocampus at stages III–IV of NFT pathology. CK1δ-positive granules commonly co-localize with p38-P **(A)**, MAP1B-P **(B)**, CAMK2A-P **(C)**, PKA α/β-P **(D)**, and tau-P Ser262 **(E)**. However, a minority of CK1-δ-positive granules are not stained with anti-p38-P **(A)** or with anti-CAMK2A-P antibodies **(C)**, and a few MAP1B-P- and PKA α/β-P-immunoreactive granules are not stained with anti-CK1-δ antibodies **(B and D**, respectively); tau-P Ser262 co-localizes with CK1-δ in the cytoplasmic granules. Nuclei are labeled with DRAQ5™ (blue). Paraffin sections, bar = 20 μm. (For interpretation of the references to colour in this figure legend, the reader is referred to the web version of this article.)

Please cite this article in press as: Andrés-Benito P et al. Dysregulated Protein Phosphorylation as Main Contributor of Granulovacuolar Degeneration at the First Stages of Neurofibrillary Tangles Pathology. Neuroscience (2021), https://doi.org/10.1016/j.neuroscience.2021.10.023

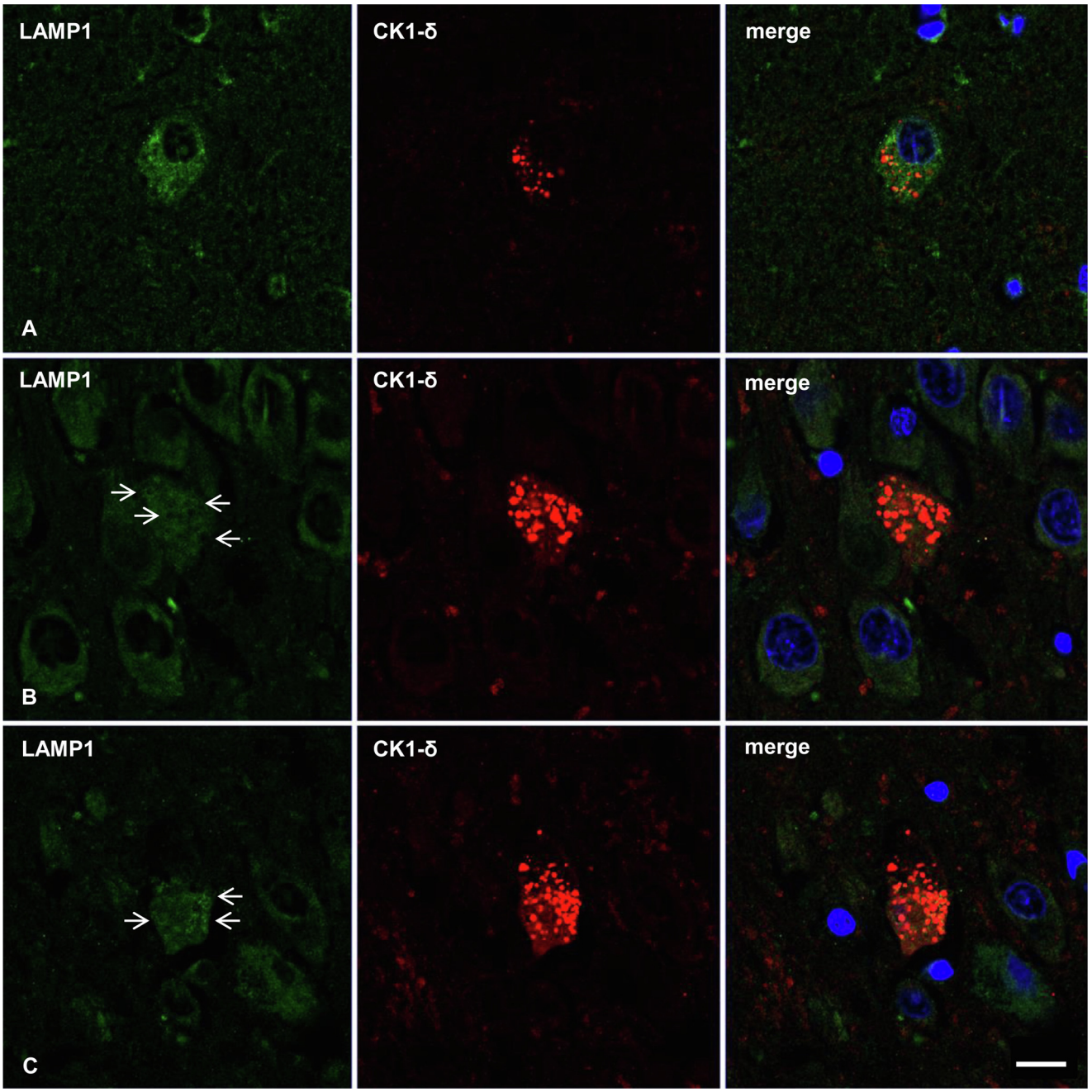

Fig. 10. Double-labeling immunofluorescence and confocal microscopy of LAMP1 (green) and CK1-δ (red) in the hippocampus at stages I–II **(A)**, II–IV **(B)**, and V–VI **(C)**. CK1-δ-immunoreactive granules are not surrounded by LAMP1-immunoreactive vacuoles but show diffuse increased cytoplasmic LAMP1 immunoreactivity. This changes may represent early stages of GVD **(A)**. Other neurons show numerous CK1-δ-immunoreactive granules surrounded by LAMP1-immunoreactive membranes **(B, C)** (arrows). However, only a minority of granules are encircled by membranes. Nuclei are labeled with DRAQ5™ (blue). Paraffin sections, bar = 30 μm. (For interpretation of the references to colour in this figure legend, the reader is referred to the web version of this article.)

FINANCIAL DISCLOSURE AND CONFLICT OF INTERESTS

No relevant data.

ETHICS APPROVAL AND CONSENT TO PARTICIPATE

Post-mortem samples were obtained from the Institute of Neuropathology HUB-ICO-IDIBELL Biobank following the guidelines of Spanish legislation on this matter and the approval of the CEIC of the Bellvitge University Hospital.

ACKNOWLEDGEMENTS

We wish to thank Tom Yohannan for editorial help.

Please cite this article in press as: Andrés-Benito P et al. Dysregulated Protein Phosphorylation as Main Contributor of Granulovacuolar Degeneration at the First Stages of Neurofibrillary Tangles Pathology. Neuroscience (2021), https://doi.org/10.1016/j.neuroscience.2021.10.023

REFERENCES

Aberle H, Bauer A, Stappert J, Kispert A, Kemler R (1997) β-catenin is a target for the ubiquitin-proteasome pathway. EMBO J 16:3797–3804.

An W-L, Cowburn RF, Li L, Braak H, Alafuzoff I, Iqbal K, Iqbal I-G, Winblad B, Pei J-J (2003) Up-regulation of phosphorylated/activated p70 S6 kinase and its relationship to neurofibrillary pathology in Alzheimer's disease. Am J Pathol 163:591–607.

Arendt T, Holzer M, Großmann A, Zedlick D, Brückner MK (1995) Increased expression and subcellular translocation of the mitogen activated protein kinase kinase and mitogen activated protein kinase in Alzheimer's disease. Neuroscience 68:5–18.

Atzori C, Ghetti B, Piva R, Srinivasan AN, Zolo P, Delisle MB, Mirra SS, Migheli A (2001) Activation of the JNK/p38 pathway occurs in diseases characterized by tau protein pathology and is related to tau phosphorylation but not to apoptosis. J Neuropathol Exp Neurol 60:1190–1197.

Barrachina M, Maes T, Buesa C, Ferrer I (2006) Lysosome associated membrane protein 1 (LAMP-1) in Alzheimer's disease. Neuropathol Appl Neurobiol 32:505–516.

Bhaskar K, Yen S-H, Lee G (2005) Disease-related modifications in tau affect the interaction between Fyn and Tau. J Biol Chem 280:35119–35125.

Bondareff W, Wischik CM, Novak M, Roth M (1991) Sequestration of tau by granulovacuolar degeneration in Alzheimer's disease. Am J Pathol 139:641–647.

Borghi R, Giliberto L, Assini A, Delacourte A, Perry G, Smith MA, Strocchi P, Zaccheo D, Tabaton M (2002) Increase of cdk5 is related to neurofibrillary pathology in progressive supranuclear palsy. Neurology 58:589–592.

Braak H, Alafuzoff I, Arzberger T, Kretzschmar H, Del Tredici K (2006) Staging of Alzheimer disease-associated neurofibrillary pathology using paraffin sections and immunocytochemistry. Acta Neuropathol 112:389–404.

Braak H, Braak E (1991) Neuropathological staging of Alzheimer-related changes. Acta Neuropathol 82:239–259.

Braak H, Braak E (1995) Staging of Alzheimer's disease-related neurofibrillary tangles. Neurobiol Aging 16:271–278.

Braak H, Del Tredici K (2011) The pathological process underlying Alzheimer's disease in individuals under thirty. Acta Neuropathol 121:171–181.

Braak H, Del Tredici K (2015) The preclinical phase of the pathological process underlying sporadic Alzheimer's disease. Brain 138:2814–2833.

Braak H, Thal DR, Ghebremedhin E, Del Tredici K (2011) Stages of the pathologic process in Alzheimer disease: age categories from 1 to 100 years. J Neuropathol Exp Neurol 70:960–969.

Buée L, Bussière T, Buée-Scherrer V, Delacourte A, Hof PR (2000) Tau protein isoforms, phosphorylation, and role in neurodegenerative disorders. Brain Res Brain Res Rev 33:95–130.

Castellani RJ, Gupta Y, Sheng B, Siedlak SL, Harris PLR, Coller JM, Perry G, Lee H-G, Tabaton M, Smith MA, Wang X, Zhu X (2011) A novel origin for granulovacuolar degeneration in aging and Alzheimer's disease: parallels to stress granules. Lab Invest 91:1777–1786.

Chalmers KA, Love S (2007) Neurofibrillary tangles may interfere with Smad 2/3 signaling in neurons. J Neuropathol Exp Neurol 66:158–167.

Chen Y, Xu J, Zhou X, Liu S, Zhang Y, Ma S, Fu AKY, Ip NY, Chen Y (2019) Changes in protein phosphorylation are associated with synaptic functions during the early stage of Alzheimer's disease. ACS Chem Neurosci 10:3986–3996.

Chin JY, Knowles RB, Schneider A, Drewes G, Mandelkow E-M, Hyman BT (2000) Microtubule-affinity regulating kinase (MARK) is tightly associated with neurofibrillary tangles in Alzheimer brain: a fluorescence resonance energy transfer study. J Neuropathol Exp Neurol 59:966–971.

Dammer EB, Lee AK, Duong DM, Gearing M, Lah JJ, Levey AI, Seyfried NT (2015) Quantitative phosphoproteomics of Alzheimer's disease reveals cross-talk between kinases and small heat shock proteins. Proteomics 15:508–519.

Dickson DW, Liu WK, Kress Y, Ku J, DeJesus O, Yen SH (1993) Phosphorylated tau immunoreactivity of granulovacuolar bodies (GVB) of Alzheimer's disease: localization of two amino terminal tau epitopes in GVB. Acta Neuropathol 85:463–470.

Drummond E, Pires G, MacMurray C, Askenazi M, Nayak S, Bourdon M, Safar J, Ueberheide N, Wisniewski T (2020) Phosphorylated tau interactome in the human Alzheimer's disease brain. Brain 143:2803-2817.

Ferrer I (2004) Stress kinases involved in tau phosphorylation in Alzheimer's disease, tauopathies and APP transgenic mice. Neurotox Res 6:469–475.

Ferrer I (2012) Defining Alzheimer as a common age-related neurodegenerative process not inevitably leading to dementia. Prog Neurobiol 97:38–51.

Ferrer I (2014) Brain banking. In: Aminoff MJ and Daroff RB, eds. Encyclopedia of the neurological sciences, 2nd edition, vol. 1. Academic Press, pp: 467-473.

Ferrer I, Andrés-Benito P (2020) White matter alterations in Alzheimer's disease without concomitant pathologies. Neuropathol Appl Neurobiol 46:654–672.

Ferrer I, Andrés-Benito P, Ausín K, Pamplona R, Rio JA, Fernández-Irigoyen J, Santamaría E (2021) Dysregulated protein phosphorylation: a determining condition in the continuum of brain aging and Alzheimer's disease. Brain Pathol 31. https://doi.org/10.1111/bpa.12996.

Ferrer I, Barrachina M, Puig B (2002) Glycogen synthase kinase-3 is associated with neuronal and glial hyperphosphorylated tau deposits in Alzheimer's disease, Pick's disease, progressive supranuclear palsy and corticobasal degeneration. Acta Neuropathol 104:583–591.

Ferrer I, Blanco R, Carmona M, Puig B (2001a) Phosphorylated mitogen-activated protein kinase (MAPK/ERK-P), protein kinase of 38 kDa (p38-P), stress-activated protein kinase (SAPK/JNK-P), and calcium/calmodulin-dependent kinase II (CaM kinase II) are differentially expressed in tau deposits in neurons and glial cells in tauopathies. J Neural Transm 108:1397–1415.

Ferrer I, Blanco R, Carmona M, Ribera R, Goutan E, Puig B, Rey MJ, Cardozo A, Viñals F, Ribalta T (2001b) Phosphorylated MAP kinase (ERK1, ERK2) expression is associated with early tau deposition in neurones and glial cells, but not with increased nuclear DNA vulnerability and cell death, in Alzheimer disease, Pick's disease, progressive supranuclear palsy and corticobasal degeneration. Brain Pathol 11:144–158.

Ferrer I, Gomez-Isla T, Puig B, Freixes M, Ribé E, Dalfó E, Avila J (2005) Current advances on different kinases involved in tau phosphorylation, and implications in Alzheimer's disease and tauopathies. Curr Alzheimer Res 2:3–18.

Ferrer I, López-González I, Carmona M, Arregui L, Dalfó E, Torrejón-Escribano B, Diehl R, Kovacs GG (2014) Glial and neuronal tau pathology in tauopathies: characterization of disease-specific phenotypes and tau pathology progression. J Neuropathol Exp Neurol 73:81–97.

Ferrer I, Martinez A, Boluda S, Parchi P, Barrachina M (2008) Brain banks: benefits, limitations, and cautions concerning the use of post-mortem brain tissue for molecular studies. Cell Tissue Bank 9:181–194.

Feuillette S, Charbonnier C, Frebourg T, Campion D, Lecourtois M (2020) A connected network of interacting proteins is involved in human-tau toxicity in *Drosophila*. Front Neurosci 14:68.

Funk KE, Kuret J (2012) Lysosomal fusion dysfunction as a unifying hypothesis for Alzheimer's disease pathology. Int J Alzheimers Dis 2012 752894.

Funk KE, Mrak RE, Kuret J (2011) Granulovacuolar degeneration (GVD) bodies of Alzheimer's disease (AD) resemble late-stage autophagic organelles. Neuropathol Appl Neurobiol 37:295-306.

Galloway PG, Perry G, Gambetti P (1987) Hirano body filaments contain actin and actin-associated proteins. J Neuropathol Exp Neurol 46:185–199.

Please cite this article in press as: Andrés-Benito P et al. Dysregulated Protein Phosphorylation as Main Contributor of Granulovacuolar Degeneration at the First Stages of Neurofibrillary Tangles Pathology. Neuroscience (2021), https://doi.org/10.1016/j.neuroscience.2021.10.023

Ghanevati M, Miller CA (2005) Phospho-beta-catenin accumulation in Alzheimer's disease and in aggresomes attributable to proteasome dysfunction. J Mol Neurosci 25:79–94.

Goedert M, Spillantini MG, Cairns NJ, Crowther RA (1992) Tau proteins in Alzheimer paired helical filaments: abnormal phosphorylation of all six brain isoforms. Neuron 8:159–168.

Goedert M, Wischik CM, Crowther RA, Walker JE, Klug A (1988) Cloning and sequencing of the cDNA encoding a core protein of the paired helical filament of Alzheimer disease: identification as microtubule-associated protein tau. Proc Natl Acad Sci U S A 85:4051–4055.

Ghoshal N, Smiley JF, DeMaggio AJ, Hoekstra MF, Cochran EJ, Binder LI, Kuret J (1999) A new molecular link between the fibrillar and granulovacuolar lesions of Alzheimer's disease. Am J Pathol 155:1163–1172.

Gunawardana CG, Mehrabian M, Wang X, Mueller I, Lubambo IB, Jonkman JEN, Wang H, Schmitt-Ulms G (2015) The Human Tau interactome: binding to the ribonucleoproteome, and impaired binding of the proline-to-leucine mutant at position 301 (P301L) to chaperones and the proteasome. Mol Cell Proteomics 14:3000–3014.

Hernández F, Avila J (2007) Tauopathies. Cell Mol Life Sci 64:2219–2233.

Hensley K, Floyd RA, Zheng NY, Nael R, Robinson KA, Nguyen X, Pye QN, Stewart CA, Geddes J, Markesbery WR, Patel E, Johnson GV, Bing G (1999) p38 kinase is activated in the Alzheimer's disease brain. J Neurochem 72:2053–2058.

Hondius DC, Koopmans F, Leistner C, Pita-Illobre D, Peferoen-Baert RM, Marbus F, Paliukhovich I, Li KW, Rozemuller AJM, Hoozemans JJM, Smit AB (2021) The proteome of granulovacuolar degeneration and neurofibrillary tangles in Alzheimer's disease. Acta Neuropathol 141:341–358. https://doi.org/10.1007/s00401-020-02261-4.

Hoozemans JJM, van Haastert ES, Nijholt DAT, Rozemuller AJM, Eikelenboom P, Scheper W (2009) The unfolded protein response is activated in pretangle neurons in Alzheimer's disease hippocampus. Am J Pathol 174:1241–1251.

Hoozemans JJM, Veerhuis R, Van Haastert ES, Rozemuller JM, Baas F, Eikelenboom P, Scheper W (2005) The unfolded protein response is activated in Alzheimer's disease. Acta Neuropathol 110:165–172.

Hou Xu, Watzlawik JO, Cook C, Liu C-C, Kang SS, Lin W-L, DeTure M, Heckman MG, Diehl NN, Al-Shaikh FSH, Walton RL, Ross OA, Melrose HL, Ertekin-Taner N, Bu G, Petrucelli L, Fryer JD, Murray ME, Dickson DW, Fiesel FC, Springer W (2021) Mitophagy alterations in Alzheimer's disease are associated with granulovacuolar degeneration and early tau pathology. Alzheimers Dement 17:417–430. https://doi.org/10.1002/alz.v17.310.1002/alz.12198.

Hyman BT, Phelps CH, Beach TG, Bigio EH, Cairns NJ, Carrillo MC, Dickson DW, Duyckaerts C, Frosch MP, Masliah E, Mirra SS, Nelson PT, Schneider JA, Thal DR, Thies B, Trojanowski JQ, Vinters HV, Montine TJ (2012) National Institute on Aging-Alzheimer's association guidelines for the neuropathological assessment of Alzheimer's disease. Alzheimers Dement 8:1–13.

Iqbal K, del C. Alonso A, Chen S, Chohan MO, El-Akkad E, Gong C-X, Khatoon S, Li B, Liu F, Rahman A, Tanimukai H, Grundke-Iqbal I (2005) Tau pathology in Alzheimer disease and other tauopathies. Biochim Biophys Acta 1739:198–210.

Ishizawa T, Sahara N, Ishiguro K, Kersh J, McGowan E, Lewis J, Hutton M, Dickson DW, Yen S-H (2003) Co-localization of glycogen synthase kinase-3 with neurofibrillary tangles and granulovacuolar degeneration in transgenic mice. Am J Pathol 163:1057–1067.

Kadokura Ai, Yamazaki T, Kakuda S, Makioka K, Lemere CA, Fujita Y, Takatama M, Okamoto K (2009) Phosphorylation-dependent TDP-43 antibody detects intraneuronal dot-like structures showing morphological characters of granulovacuolar degeneration. Neurosci Lett 463:87–92.

Kannanayakal TJ, Tao H, Vandre DD, Kuret J (2006) Casein kinase-1 isoforms differentially associate with neurofibrillary and granulovacuolar degeneration lesions. Acta Neuropathol 111:413–421.

Köhler C (2016) Granulovacuolar degeneration: a neurodegenerative change that accompanies tau pathology. Acta Neuropathol 132:339–359.

Köhler C, Dinekov M, Götz J (2013) Active glycogen synthase kinase-3 and tau pathology-related tyrosine phosphorylation in pR5 human tau transgenic mice. Neurobiol Aging 34:1369-1379.

Köhler C, Dinekov M, Götz J (2014) Granulovacuolar degeneration and unfolded protein response in mouse models of tauopathy and Aβ amyloidosis. Neurobiol Dis 71:169–179.

Krigman MR, Feldman RG, Bensch K (1965) Alzheimer's presenile dementia. A histochemical and electron microscopic study. Lab Invest 14:381–389.

Lagalwar S, Berry RW, Binder LI (2007) Relation of hippocampal phospho-SAPK/JNK granules in Alzheimer's disease and tauopathies to granulovacuolar degeneration bodies. Acta Neuropathol 113:63–73.

Lee HG, Ueda M, Zhu X, Perry G, Smith MA (2006) Ectopic expression of phospho-Smad2 in Alzheimer's disease: uncoupling of the transforming growth factor-beta pathway? J Neurosci Res 84:1856–1861.

Leroy K, Boutajangout A, Authelet M, Woodgett JR, Anderton BH, Brion JP (2002) The active form of glycogen synthase kinase-3beta is associated with granulovacuolar degeneration in neurons in Alzheimer's disease. Acta Neuropathol 103:91–99.

Liu WK, Williams RT, Hall FL, Dickson DW, Yen SH (1995) Detection of a Cdc2-related kinase associated with Alzheimer-paired helical filaments. Am J Pathol 146:228–238.

Love S, Saitoh T, Quijada S, Cole GM, Terry RD (1988) Alz-50, ubiquitin and tau immunoreactivity of neurofibrillary tangles, Pick bodies and Lewy bodies. J Neuropathol Exp Neurol 47:393–405.

Montine TJ, Phelps CH, Beach TG, Bigio EH, Cairns NJ, Dickson DW, Duyckaerts C, Frosch MP, Masliah E, Mirra SS, Nelson PT, Schneider JA, Thal DR, Trojanowski JQ, Vinters HV, Hyman BT; National Institute on Aging; Alzheimer's Association (2012) National Institute on Aging-Alzheimer's Association guidelines for the neuropathologic assessment of Alzheimer's disease: a practical approach. Acta Neuropathol 123:1-11.

Nakamori M, Takahashi T, Yamazaki Y, Kurashige T, Yamawaki T, Matsumoto M (2012) Cyclin-dependent kinase 5 immunoreactivity for granulovacuolar degeneration. NeuroReport 23:867–872.

Nelson PT, Alafuzoff I, Bigio EH, Bouras C, Braak H, Cairns NJ, Castellani RJ, Crain BJ, Davies P, Del Tredici K, Duyckaerts C, Frosch MP, Haroutunian V, Hof PR, Hulette CM, Hyman BT, Iwatsubo T, Jellinger KA, Jicha GA, Kövari E, Kukull WA, Leverenz JB, Love S, Mackenzie IR, Mann DM, Masliah E, McKee AC, Montine TJ, Morris JC, Schneider JA, Sonnen JA, Thal DR, Trojanowski JQ, Troncoso JC, Wisniewski T, Woltjer RL, Beach TG (2012) Correlation of Alzheimer's disease neuropathological changes with cognitive status: a review of the literature. J Neuropathol Exp Neurol 71:362–381.

Nijholt DAT, van Haastert ES, Rozemuller AJM, Scheper W, Hoozemans JJM (2012) The unfolded protein response is associated with early tau pathology in the hippocampus of tauopathies. J Pathol 226:693–702.

Okamoto K, Hirai S, Iizuka T, Yanagisawa T, Watanabe M (1991) Reexamination of granulovacuolar degeneration. Acta Neuropathol 82:340–345.

Oyanagi S, Ikuta F (1974) An ultrastructural observation on granulovacuolar degenerations in reference to the process of their formation. Brain Nerve (Tokyo) 26:783–788.

Pei J-J, Braak H, An W-L, Winblad B, Cowburn RF, Iqbal K, Grundke-Iqbal I (2002a) Up-regulation of mitogen-activated protein kinases ERK1/2 and MEK1/2 is associated with the progression of neurofibrillary degeneration in Alzheimer's disease. Brain Res Mol Brain Res 109:45–55.

Pei JJ, Braak E, Braak H, Grundke-Iqbal I, Iqbal K, Winblad B, Cowburn RF (1999) Distribution of active glycogen synthase kinase 3 (GSK-3) in brains staged for Alzheimer disease neurofibrillary changes. J Neuropathol Exp Neurol 58:1010–1019.

Please cite this article in press as: Andrés-Benito P et al. Dysregulated Protein Phosphorylation as Main Contributor of Granulovacuolar Degeneration at the First Stages of Neurofibrillary Tangles Pathology. Neuroscience (2021), https://doi.org/10.1016/j.neuroscience.2021.10.023

Pei J-J, Braak E, Braak H, Grundke-Iqbal I, Iqbal K, Winblad B, Cowburn RF (2001) Localization of active forms of c-Jun kinase (JNK) and p38 kinase in Alzheimer's disease brains at different stages of neurofibrillary degeneration. J Alzheimer's Dis 3:41–48.

Pei J-J, Braak H, Gong C-X, Grundke-Iqbal I, Iqbal K, Winblad B, Cowburn RF (2002b) Up-regulation of cell division cycle (cdc) 2 kinase in neurons with early stage Alzheimer's disease neurofibrillary degeneration. Acta Neuropathol 104:369–376.

Pei J-J, Grundke-Iqbal I, Iqbal K, Bogdanovic N, Winblad B, Cowburn RF (1998) Accumulation of cyclin-dependent kinase 5 (cdk5) in neurons with early stages of Alzheimer's disease neurofibrillary degeneration. Brain Res 797:267–277.

Pei JJ, Khatoon S, An WL, Nordlinder M, Tanaka T, Braak H, Tsujio I, Takeda M, Alafuzoff I, Winblad B, Cowburn RF, Grundke-Iqbal I, Iqbal K (2003) Role of protein kinase B in Alzheimer's neurofibrillary pathology. Acta Neuropathol 105:381-392.

Pei J-J, Tanaka T, Tung YC, Braak E, Iqbal K, Grundke-Iqbal I (1997) Distribution, levels, and activity of glycogen synthase kinase-3 in the Alzheimer disease brain. J Neuropathol Exp Neurol 56:70–78.

Perry G, Roder H, Nunomura A, Takeda A, Friedlich AL, Zhu X, Raina AL, Holbrook N, Siedlak SL, Harris PLR, Smith MA (1999) Activation of extracellular receptor kinase (ERK) in Alzheimer's disease links oxidative stress to abnormal tau phosphorylation. NeuroReport 10:2411–2415.

Rudrabhatla P, Jaffe H, Pant HC (2011) Direct evidence of phosphorylated neuronal intermediate filament proteins in neurofibrillary tangles (NFTs): phosphoproteomics of Alzheimer's NFTs. FASEB J 25:3896–3905.

Sathe G, Mangalaparthi KK, Jain A, Darrow J, Troncoso J, Albert M, Moghekar A, Pandey A (2020) Multiplexed phosphoproteomic study of brain in patients with Alzheimer's disease and age-matched cognitively healthy controls. OMICS 24:216–227.

Schwab C, DeMaggio AJ, Ghoshal N, Binder LI, Kuret J, McGeer PL (2000) Casein kinase 1δ is associated with pathological accumulation of tau in several neurodegenerative diseases. Neurobiol Aging 21:503–510.

Selznick LA, Holtzman DM, Han BH, Gökden M, Srinivasan AN, Johnson EM, Roth KA (1999) In situ immunodetection of neuronal caspase-3 activation in Alzheimer disease. J Neuropathol Exp Neurol 58:1020–1026.

Sinsky J, Majerova P, Kovac A, Kotlyar M, Jurisica I, Hanes J (2020) Physiological tau interactome in brain and its link to tauopathies. J Proteome Res 19:2429–2442.

Stadelmann C, Deckwerth TL, Srinivasan A, Bancher C, Brück W, Jellinger K, Lassmann H (1999) Activation of caspase-3 in single neurons and autophagic granules of granulovacuolar degeneration in Alzheimer's disease. Evidence for apoptotic cell death. Am J Pathol 155:1459–1466.

Stancu IC, Ferraiolo M, Terwel D, Dewachter I (2019) Tau interacting proteins: gaining insight into the roles of Tau in health and disease. Adv Exp Med Biol 1184:145–166.

Spillantini MG, Goedert M (2013) Tau pathology and neurodegeneration. Lancet Neurol 12:609–622.

Su JH, Kesslak PJ, Head E, Cotman CW (2002) Caspase cleaved amyloid precursor protein and activated caspase-3 are co-localized in the granules of granulovacuolar degeneration in Alzheimer's disease and Down's syndrome brain. Acta Neuropathol 104:1–6.

Sun A, Liu M, Nguyen XV, Bing G (2003) p38MAP kinase is activated at early stages in Alzheimer's disease brain. Exp Neurol 183:394–405.

Tagawa H, Homma H, Saito A, Fujita K, Chen XG, Imoto S, Oka T, Ito H, Motoki K, Yoshida C, Hatsuta H, Murayama S, Iwatsubo T, Miyano S, Okazawa H (2015) Comprehensive phosphoproteome analysis unravels the core signaling network that initiates the earliest synapse pathology in preclinical Alzheimer disease brain. Hum Mol Genet 24:540–558.

Tan H, Wu Z, Wang H, Bai B, Li Y, Wang X, Zhai B, Beach TG, Peng J (2015) Refined phosphopeptide enrichment by phosphate additive and the analysis of human brain phosphoproteome. Proteomics 15:500–507.

Tanida I, Ueno T, Kominami E (2008) LC3 and autophagy. Methods Mol Biol 445:77–88.

Thakur A, Wang X, Siedlak SL, Perry G, Smith MA, Zhu X (2007) c-Jun phosphorylation in Alzheimer disease. J Neurosci Res 85:1668–1673.

Thal DR, Del Tredici K, Ludolph AC, Hoozemans JJM, Rozemuller AJ, Braak H, Knippschild U (2011) Stages of granulovacuolar degeneration: their relation to Alzheimer's disease and chronic stress response. Acta Neuropathol 122:577–589.

Thal DR, Rüb U, Orantes M, Braak H (2002) Phases of A β-deposition in the human brain and its relevance for the development of AD. Neurology 58:1791–1800.

Triplett JC, Swomley AM, Cai J, Klein JB, Butterfield DA, Mecocci P (2016) Quantitative phosphoproteomic analyses of the inferior parietal lobule from three different pathological stages of Alzheimer's disease. J Alzheimers Dis 49:45–62.

Ueberham U, Ueberham E, Gruschka H, Arendt T (2006) Altered subcellular location of phosphorylated Smads in Alzheimer's disease. Eur J Neurosci 24:2327-2334.

Unterberger U, Höftberger R, Gelpi E, Flicker H, Budka H, Voigtländer T (2006) Endoplasmic reticulum stress features are prominent in Alzheimer disease but not in prion diseases in vivo. J Neuropathol Exp Neurol 65:348–357.

Vincent I, Jicha G, Rosado M, Dickson DW (1997) Aberrant expression of mitotic cdc2/cyclin B1 kinase in degenerating neurons of Alzheimer's disease brain. J Neurosci 17:3588–3598.

Wegiel J, Dowjat K, Kaczmarski W, Kuchna I, Nowicki K, Frackowiak J, Mazur Kolecka B, Wegiel J, Silverman WP, Reisberg B, deLeon M, Wisniewski T, Gong C-X, Liu F, Adayev T, Chen-Hwang M-C, Hwang Y-W (2008) The role of overexpressed DYRK1A protein in the early onset of neurofibrillary degeneration in Down syndrome. Acta Neuropathol 116:391–407.

Wiersma VI, Scheper W (2020) Granulovacuolar degeneration bodies: red alert for neurons with MAPT/tau pathology. Autophagy 16:173–175.

Wiersma VI, van Ziel AM, Vazquez-Sanchez S, Nölle A, Berenjeno-Correa E, Bonaterra-Pastra A, Clavaguera F, Tolnay M, Musters RenéJP, van Weering JRT, Verhage M, Hoozemans JJM, Scheper W (2019) Granulovacuolar degeneration bodies are neuron-selective lysosomal structures induced by intracellular tau pathology. Acta Neuropathol 138:943–970.

Yamaguchi H, Ishiguro K, Uchida T, Takashima A, Lemere CA, Imahori K (1996) Preferential labeling of Alzheimer neurofibrillary tangles with antisera for tau protein kinase (TPK) I/glycogen synthase kinase-3 and cyclin-dependent kinase 5, a component of TPK II. Acta Neuropathol 92:232–241.

Yamazaki Y, Matsubara T, Takahashi T, Kurashige T, Dohi E, Hiji M, Nagano Y, Yamawaki T, Matsumoto M, Duda J (2011) Granulovacuolar degenerations appear in relation to hippocampal phosphorylated tau accumulation in various neurodegenerative disorders. PLoS One 6:e26996.

Yamazaki Y, Takahashi T, Hiji M, Kurashige T, Izumi Y, Yamawaki T, Matsumoto M (2010) Immunopositivity for ESCRT-III subunit CHMP2B in granulovacuolar degeneration of neurons in the Alzheimer's disease hippocampus. Neurosci Lett 477:86–90.

Zahid S, Oellerich M, Asif AR, Ahmed N (2012) Phosphoproteome profiling of substantia nigra and cortex regions of Alzheimer's disease patients. J Neurochem 121: 954-963.

Zhu X, Castellani RJ, Takeda A, Nunomura A, Atwood CS, Perry G, Smith MA (2001a) Differential activation of neuronal ERK, JNK/SAPK and p38 in Alzheimer's disease, the two hit hypothesis. Mech Ageing Dev 123:39–46.

Zhu X, Lee HG, Raina AK, Perry G, Smith MA (2002) The role of mitogen-activated protein kinase pathways in Alzheimer's disease. Neurosignals 11:270–281.

Zhu X, Ogawa O, Wang Y, Perry G, Smith MA (2003a) JKK1, an upstream activator of JNK/SAPK, is activated in Alzheimer's disease. J Neurochem 85:87–93.

Zhu X, Raina AK, Rottkamp CA, Aliev G, Perry G, Boux H, Smith MA (2001b) Activation and redistribution of c-Jun N-terminal kinase/

Please cite this article in press as: Andrés-Benito P et al. Dysregulated Protein Phosphorylation as Main Contributor of Granulovacuolar Degeneration at the First Stages of Neurofibrillary Tangles Pathology. Neuroscience (2021), https://doi.org/10.1016/j.neuroscience.2021.10.023

stress activated protein kinase in degenerating neurons in Alzheimer's disease. J Neurochem 76:435–441.

Zhu X, Rottkamp CA, Boux H, Takeda A, Perry G, Smith MA (2000) Activation of p38 kinase links tau phosphorylation, oxidative stress, and cell cycle-related events in Alzheimer disease. J Neuropathol Exp Neurol 59:880–888.

Zhu X, Rottkamp CA, Hartzler A, Sun Z, Takeda A, Boux H, Shimohama S, Perry G, Smith MA (2001c) Activation of MKK6, an upstream activator of p38, in Alzheimer's disease. J Neurochem 79:311–318.

Zhu X, Sun Z, Lee HG, Siedlak SL, Perry G, Smith MA (2003b) Distribution, levels, and activation of MEK1 in Alzheimer's disease. J. Neurochem 86:136–142.

APPENDIX A. SUPPLEMENTARY DATA

Supplementary data to this article can be found online at https://doi.org/10.1016/j.neuroscience.2021.10.023.

(Received 21 June 2021, Accepted 21 October 2021)
(Available online xxxx)